Journal of Cellular Physiology

The Paracrine Feedback Loop Between Vitamin D_3 (1,25 $(OH)_2D_3$) and PTHrP in Prehypertrophic Chondrocytes

FRANCES C. BACH,[1]* KIRSTEN RUTTEN,[1] KRISTYANNE HENDRIKS,[1] FRANK M. RIEMERS,[1] PETER CORNELISSEN,[2] ALAIN DE BRUIN,[2] GER J. ARKESTEIJN,[3] RICHARD WUBBOLTS,[4] WILLIAM A. HORTON,[5,6] LOUIS C. PENNING,[1] AND MARIANNA A. TRYFONIDOU[1]

[1]*Faculty of Veterinary Medicine, Department of Clinical Sciences of Companion Animals, Utrecht University, Utrecht, The Netherlands*

[2]*Faculty of Veterinary Medicine, Department of Pathobiology, Utrecht University, Utrecht, The Netherlands*

[3]*Faculty of Veterinary Medicine, Department of Immunology, Utrecht University, Utrecht, The Netherlands*

[4]*Faculty of Veterinary Medicine, Department of Biochemistry and Cell Biology, Utrecht University, Utrecht, The Netherlands*

[5]*Research Center, Shriners Hospital for Children, Portland, Oregon*

[6]*Department of Molecular and Medical Genetics, Oregon Health and Science University, Portland, Oregon*

The endocrine feedback loop between vitamin D_3 ($1,25(OH)_2D_3$) and parathyroid hormone (PTH) plays a central role in skeletal development. PTH-related protein (PTHrP) shares homology and its receptor (PTHR1) with PTH. The aim of this study was to investigate whether there is a functional paracrine feedback loop between $1,25(OH)_2D_3$ and PTHrP in the growth plate, in parallel with the endocrine feedback loop between $1,25(OH)_2D_3$ and PTH. This was investigated in ATDC5 cells treated with 10^{-8} M $1,25(OH)_2D_3$ or PTHrP, Col2-pd2EGFP transgenic mice, and primary Col2-pd2EGFP growth plate chondrocytes isolated by FACS, using RT-qPCR, Western blot, PTHrP ELISA, chromatin immunoprecipitation (ChIP) assay, silencing of the $1,25(OH)_2D_3$ receptor (VDR), immunofluorescent staining, immunohistochemistry, and histomorphometric analysis of the growth plate. The ChIP assay confirmed functional binding of the VDR to the PTHrP promoter, but not to the PTHR1 promoter. Treatment with $1,25(OH)_2D_3$ decreased PTHrP protein production, an effect which was prevented by silencing of the VDR. Treatment with PTHrP significantly induced VDR production, but did not affect 1α- and 24-hydroxylase expression. Hypertrophic differentiation was inhibited by PTHrP and 1,25 $(OH)_2D_3$ treatment. Taken together, these findings indicate that there is a functional paracrine feedback loop between $1,25(OH)_2D_3$ and PTHrP in the growth plate. $1,25(OH)_2D_3$ decreases PTHrP production, while PTHrP increases chondrocyte sensitivity to 1,25 $(OH)_2D_3$ by increasing VDR production. In light of the role of $1,25(OH)_2D_3$ and PTHrP in modulating chondrocyte differentiation, 1,25 $(OH)_2D_3$ in addition to PTHrP could potentially be used to prevent undesirable hypertrophic chondrocyte differentiation during cartilage repair or regeneration.

J. Cell. Physiol. 229: 1999–2014, 2014.

Abbreviations: 1α-OHase, 1α-hydroxylase; 24-OHase, 24-hydroxylase; AsAP, ascorbic acid 2-phosphate; bp, base pairs; BMSC, bone marrow-derived stem cells; BW, body weight; Ca, calcium; ChIP, chromatin immunoprecipitation; Col2a1, collagen type 2; Col9, collagen type 9; ColX, collagen type X; FACS, fluorescence-activated cell sorting; FBS, fetal bovine serum; GPI.Th, mean growth plate height; GPI.$Th._{Pr}$, mean height of the proliferative growth plate zone; GPI.$Th._{Hp}$, mean height of the hypertrophic growth plate zone; HRP, horseradish peroxidase; Mab, monoclonal antibody; MSC, mesenchymal stem cell; n.s., not significant; OA, osteoarthritis; P, inorganic phosphate; Pab, polyclonal antibody; PTH, parathyroid hormone; PTHrP, PTH-related protein; PTHR1, PTH/PTHrP receptor; RT, room temperature; SD, standard deviation; siRNA, silencing RNA; Tm, melting temperature; TSS, transcription start site; VDR, nuclear vitamin D3 receptor; VDRE, vitamin D3 response element.

The authors declare that they have no competing interests.

Contract grant sponsor: Dutch Arthritis Foundation;
Contract grant number: LLP22.
Contract grant sponsor: NWO (MEERVOUD grant);
Contract grant number: 836.07.003.

Correspondence to: Frances Bach, Faculty of Veterinary Medicine, Department of Clinical Sciences of Companion Animals, Utrecht University, Yalelaan 108, 3508 TD Utrecht, The Netherlands.
E-mail: f.c.bach@uu.nl

Manuscript Received: 14 February 2014
Manuscript Accepted: 25 April 2014

Accepted manuscript online in Wiley Online Library (wileyonlinelibrary.com): 29 April 2014.
DOI: 10.1002/jcp.24658

Longitudinal bone growth occurs at the growth plate, a highly organized cartilage structure that contains proliferating chondrocytes. These cells undergo a maturation process involving hypertrophy followed by apoptosis, thereby facilitating bone formation (Nilsson et al., 2005; Brochhausen et al., 2009). Some changes that occur in cartilage after injury or osteoarthritis (OA) resemble the processes that occur during the differentiation of growth plate chondrocytes (Dreier, 2010; Zhang et al., 2012). In healthy articular cartilage, chondrocytes resist proliferation and terminal differentiation. In contrast, cartilage damage caused by injuries or OA reactivates chondrocyte hypertrophy as part of a repair mechanism, accompanied by acquisition of an autolytic phenotype and cartilage degradation (Dreier, 2010; van der Kraan and van den Berg, 2012; Zhang et al., 2012). Ultimately, the hypertrophic chondrocytes undergo apoptosis to enable bone deposition (van der Kraan and van den Berg, 2012). The inferior quality of the repaired cartilage suggests that the inhibition of chondrocyte hypertrophy could be a target of treatment to improve cartilage repair (Zhang et al., 2012).

Chondrocyte proliferation and differentiation at the growth plate is regulated through the interaction of systemic hormones (endocrine level) and locally produced growth factors (autocrine and/or paracrine level). The endocrine feedback loop between the active metabolite of vitamin D_3 ($1,25(OH)_2D_3$) and parathyroid hormone (PTH) plays a central role in calcium and phosphate homeostasis during skeletal growth (Nilsson et al., 2005). Vitamin D_3 is hydroxylated in the liver to 25-hydroxycholecalciferol ($25(OH)D_3$), which is thereafter hydroxylated in various target cells into $1,25(OH)_2D_3$ by the enzyme 1α-hydroxylase (St-Arnaud and Naja, 2011). $1,25(OH)_2D_3$ in turn can be deactivated and catabolized by the enzyme 24-hydroxylase (Akeno et al., 1997; Tryfonidou et al., 2003). It has been shown that $1,25(OH)_2D_3$ exerts its genomic effects by binding to its nuclear receptor (VDR), and that this complex then binds to vitamin D_3 response elements (VDREs) in the promoter region of various target genes (Healy et al., 2003,2005b; St-Arnaud and Naja, 2011).

Both $1,25(OH)_2D_3$ and PTH are also active at the growth plate and play an important autocrine and/or paracrine role during chondrocyte proliferation and/or differentiation (Kato et al., 1990; Klaus et al., 1991; Drissi et al., 2002). Growth plate chondrocytes express the VDR and the enzymes 1α- and 24-hydroxylase in vitro as well as in vivo (Boyan et al., 2002; Hugel et al., 2004; Nilsson et al., 2005; Naja et al., 2009; St-Arnaud and Naja, 2011). PTH-related protein (PTHrP) resembles PTH in genetic sequence and structure and both PTH and PTHrP share the same receptor: PTHR1 (Schipani and Provot, 2003; Zhang et al., 2012). PTHR1 is expressed in low levels by proliferating chondrocytes and in high levels by pre/early hypertrophic chondrocytes (Kronenberg, 2003; Mak et al., 2008; Zhang et al., 2012). PTHrP is produced by proliferative growth plate chondrocytes and prevents proliferative cells from leaving the proliferating pool. In this way, hypertrophic chondrocyte differentiation is delayed (Kronenberg, 2003; Mak et al., 2008; Hirai et al., 2011; Zhang et al., 2012).

Understanding the processes behind chondrocyte differentiation is crucial, not only from a developmental point of view. Regenerative strategies for bone and cartilage make use of mesenchymal (stem) cells undergoing chondrogenic differentiation. The growth plate can be used as a model to study these processes, mainly because it has a highly organized structure, with chondrocytes undergoing differentiation in an orderly fashion (Nilsson et al., 2005; Brochhausen et al., 2009; Denison et al., 2009). Therefore, the main aim of this study was to investigate whether there is a functional paracrine feedback loop between $1,25(OH)_2D_3$ and PTHrP in prehypertrophic growth plate chondrocytes, in parallel to the well-known endocrine $1,25(OH)_2D_3$-PTH feedback loop.

We hypothesized that PTHrP increases the sensitivity of growth plate chondrocytes to $1,25(OH)_2D_3$ either by increasing $1,25(OH)_2D_3$ production by upregulating 1α-hydroxylase, and/or decreasing the catabolism of $1,25(OH)_2D_3$ by downregulating 24-hydroxylase, and/or by upregulating VDR expression (Supplementary File 1). The feedback loop is closed by the inhibition of PTHrP and/or PTHR1 transcription by the binding of $1,25(OH)_2D_3$ to a VDRE located in the promoter region of (one of) these target genes.

Materials and Methods

In vitro studies with the ATDC5 cell line

Cell culture and experimental design. The mouse chondrogenic ATDC5 cell line was kindly provided by Dr. T. Welting (UMC Maastricht, The Netherlands). Cell culture was performed as described previously (Caron et al., 2012). Standard differentiation culture medium was supplemented with 0.2 mM L-ascorbic acid 2-phosphate (AsAP, A8960, Sigma-Aldrich, Saint Louis) to reduce the time in culture until prehypertrophic differentiation (Altaf et al., 2006). Cells grown in a standard differentiation medium were compared with cells grown in a standard differentiation medium supplemented with 10^{-8} M PTHrP (pTH-Related Protein (1–34) amide, H-9095, Bachem, Bubendorf, Switzerland) or 10^{-8} M $1,25(OH)_2D_3$ (kindly provided by Dr. C. Veldhuizen, Dishman, The Netherlands). Stripped fetal bovine serum (FBS) was used, which is devoid of vitamin D_3 metabolites and growth factors. ATDC5 cells were plated on 24-well plates (Greiner Cellstar®) at a density of 6,400 cells/cm^2. Six hours later, cell differentiation was induced (day 0). The three different culture groups were studied from differentiation day 7 until day 10 (prehypertrophic phase) at the following time points: T_0, T_1, T_2, T_4, T_8, T_{24}, T_{28}, T_{48}, and T_{72} (the digits indicate the number of hours after PTHrP or $1,25(OH)_2D_3$ was first added to the cell culture medium). A T_0, T_{24}, and T_{48}, 10^{-8} M PTHrP or $1,25(OH)_2D_3$ was added to the experimental plates. The experiment was repeated at least six times for each time point and culture condition.

RNA isolation and cDNA synthesis. Total RNA was extracted with the aid of the RNeasy® Mini kit (74104, Qiagen, Valencia, CA), according to the manufacturer's protocol. An additional DNA digestion step with DNase (RNAse-Free DNase Set, 79254, Qiagen) was included to ensure DNA removal. Total RNA was quantified with a Nanodrop® ND-1000 spectrophotometer (Thermo Scientific, Wilmington, DE). cDNA was synthesized using the iScript™ cDNA Synthesis Kit (170-8891, Bio-Rad, Veenendaal, The Netherlands), according to the manufacturer's instructions.

Quantitative determination of the expression of target genes. Primer nucleotide sequences for all reference genes were obtained from the Eccles Lab Reference Gene List (http://openwetware.org/wiki/Eccles:QPCR_reference_genes). Most primer nucleotide sequences for the target genes were obtained from PrimerBank (http://pga.mgh.harvard.edu/primerbank/index.html). For the other target genes, primer sequences were designed using PerlPrimer (http://perlprimer.sourceforge.net). Subsequently, M-fold version 3.2 was used to check for secondary structure formation (Zuker, 2003). Primer uniqueness and specificity was determined using BLAST (Altschul et al., 1997). Annealing temperatures were established by performing a temperature gradient PCR on a 16-fold dilution series. Amplicons were validated by sequence analysis using an ABI Prism 3130XL genetic analyzer (Applied Biosystems, Foster City, CA). All primers were purchased from Eurogentec (Maastricht, The Netherlands). An overview of the primer pairs used is given in Supplementary File 2. In order to normalize the relative expression of the target genes, a set of 10 reference genes was evaluated:

Hspca, *Rpl32*, *Rps19*, *Ywhaz*, *B2m*, *Gapdh*, *Hbms*, *Hprt-1*, *Sdha*, and *Tbp*. The geNorm program was used to evaluate the stability of the housekeeping genes (Vandesompele et al., 2002). The three most stably expressed reference genes in the ATDC5 cell line, *Rpl32*, *Rps1*, and *Sdha*, were chosen to normalize gene expression. However, *Sdha* was not used as a reference gene in the experiment in which the VDR was silenced, because *Sdha* gene expression was not sufficiently stable under the experimental conditions used. RT-qPCR was performed using the iQ™ SYBR Green Supermix Kit (Bio-Rad, Veenendaal, The Netherlands) and the MyiQ™ single color Real-Time PCR Detection System (Bio-Rad).

Protein isolation and Western blot. Semi-quantitative protein expression of the VDR and collagen type X was determined using Western blot. Protein was extracted from the ATDC5 cells with 50 μl RIPA buffer per well, and protein concentration was determined with a Lowry assay (500-0116, Bio-Rad). Thereafter, 30 μg protein was subjected to 12% SDS–PAGE, and electroblotted onto a Hybond-C nitrocellulose membrane (90RPN203C, GE Healthcare Life Sciences, Diegem, Belgium). Only one SDS–PAGE gel and membrane was used per target protein. The membrane was blocked for 60 min, followed by overnight incubation at 4°C with the first antibody (Supplementary File 3). Thereafter, the membrane was washed and incubated for 60 min with a horseradish peroxidase (HRP)-conjugated second antibody. Protein was detected by enhanced chemiluminescence (Molecular Imager ChemiDoc XRS System, Bio-Rad). Control experiments were included in which the first antibody was omitted. After completion of Western blotting of the target proteins, the membranes were stripped using Stripping Buffer (Restore™ Western Blot Stripping Buffer, 21059, Thermo Scientific), and β-actin protein expression was determined. The mean volume of the protein bands was determined with Quantity One software using volumetric band analysis. The mean volume of the target gene was divided by the mean volume of β-actin (target gene/β-actin ratio), to correct for different protein concentrations applied to the membranes. Western blot images were prepared using Adobe Photoshop CS5.1. Linear adjustment of brightness, contrast, and color balance was applied to every pixel in the image.

PTHrP ELISA. The concentration of PTHrP in the cell lysate and culture media (which was stored at −70°C) was measured with an ELISA (ELISA kit for mouse PLP, USCN E90819Mu), according to the manufacturer's instructions.

mRNA superinduction. RNA and protein samples were taken from the control cultures and the 10^{-8} M $1,25(OH)_2D_3$-treated cultures on differentiation day 7 at T_0, T_1, T_2, T_4, T_8, T_{12}, and T_{24}. RNA isolation, cDNA synthesis, RT-qPCR for *Pthrp* and a PTHrP ELISA were performed as described previously.

DNA quantification. DNA was quantified using the Quant-iT™ PicoGreen® dsDNA Assay Kit (P11496, Invitrogen, Paisley, UK).

Silencing RNA. Stealth RNAi™ siRNA Duplex (10620312, Invitrogen) was used to silence the ATDC5 VDR. The siRNA oligonucleotide sequence used for the mouse VDR (nm_009504) was: 5′ CCCUUCAAUGGAGAUUGCCGCAUCA 3′ (ORF, GC percentage estimated at 52%). A Stealth RNAi™ Control Duplex (Invitrogen) sequence 5′ CCCUAACGAGGGUUA CGCCAUUUCA 3′ (scrambled mock, GC percentage estimated at 52%) was used to determine the effect of Stealth RNAi™ siRNA Duplex versus background. Lipofectamine™ RNAiMAX (13778-075, Invitrogen) was used as transfection reagent. ATDC5 cells were plated on 24-well plates (Greiner Cellstar®) at a standard density of 6,400 /cm^2. Six hours later, ATDC5 cell differentiation was induced (day 0). On differentiation day 4, RNA in the approximately 100% confluent ATDC5 cells was silenced (Lipofectamine™ RNAiMAX concentration of 5.3 μl/ml, siRNA VDR-oligo (Stealth RNAi™ siRNA Duplex)/scrambled mock (Stealth RNAi™ siRNA Control Duplex) concentration of 50 nM). After siRNA transfection medium was added to the experimental plates, the ATDC5 cells were incubated for 48 h at 37°C in 5% CO_2 before the siRNA transfection medium was replaced by normal differentiation medium. On day 7 of differentiation (which was 72 h after siRNA initiation), 10^{-8} M PTHrP or $1,25(OH)_2D_3$ was added to determine whether the effects of PTHrP and $1,25(OH)_2D_3$ on the ATDC5 cells could be prevented by VDR silencing. From differentiation day 7 until day 10 (i.e., 72–144 h after siRNA initiation), the different culture groups were studied at the time points T_0, T_{24}, T_{48}, and T_{72} (the digits indicate the number of hours after PTHrP or $1,25(OH)_2D_3$ was first added to the cell culture medium). 10^{-8} M PTHrP or $1,25(OH)_2D_3$ was added at T_0, T_{24}, and T_{48}. Nine different cell culture conditions (control, control + scrambled mock, control + VDR-oligo, PTHrP, PTHrP + scrambled mock, PTHrP + VDR-oligo, $1,25(OH)_2D_3$, $1,25(OH)_2D_3$ + scrambled mock, and $1,25(OH)_2D_3$ + VDR-oligo) were studied and compared.

Chromatin immunoprecipitation (ChIP) assay. The sequence and location of the VDREs in the PTHrP promoter region have only been determined in the rat (Falzon, 1996; Kremer et al., 1996a). The *Mus musculus* and *Rattus norvegicus* PTHrP promoter regions were BLASTed (Altschul et al., 1997) to determine their homology (Supplementary File 4). Primers were designed and validated for the two VDRE regions of the mouse PTHrP promoter (Supplementary File 4, Fig. 3A). As a negative control, primers were designed at 1,000 bp upstream of VDRE2.

To date, there is no VDRE reported for the PTHR1 gene. The PTHR1 gene has two promoter regions, P1 and P2 (Fig. 3C). In bone and cartilage, the P2 promoter controls *Pthr1* gene expression, and therefore we searched for possible VDREs in this P2 promoter with the aid of the core binding motif consensus sequence RGKTSA (R=A or G, K=G or T, S=C or G) (Toell et al., 2000). This motif was included in two six-nucleotide sequences in the region upstream of U3: AGGTGA and GGTTGA, which are 2,092 and 2,027 bp upstream of the transcription start site (TSS), respectively. The distance between these sequences was 104 bp. The consensus is that a VDRE has normally three to six nucleotides between the two motif sequences (Carlberg, 1995). We cannot exclude that the area between these two sequences loops back to bring the sequences close together, enabling the VDR to bind. For this reason, primers were designed for each six-nucleotide sequence (VDRE1 and VDRE2), but also for the region containing these two core binding motif consensus sequences (VDRE combination). As negative and positive controls, primers were designed at 1,000 bp upstream of the expected VDREs and for one of the VDREs of the 24-hydroxylase promoter, respectively (Supplementary File 4). VDREs for 24-hydroxylase have been identified in the rat (Zierold et al., 1995), and therefore the rat promoter region was BLASTed against the mouse 24-hydroxylase promoter region. Both VDREs revealed 100% alignment. Primers were designed for the VDRE 5′ CGCACCCGCTGAACC 3′.

The ChIP assay was performed as described previously (Pandit et al., 2012), with minor modifications. Briefly, ATDC5 cells were seeded in Falcon Primaria petri dishes (353803, BD Biosciences, Breda, The Netherlands) at a density of 6,400 cells/cm^2 and cultured for 7 days (approximately 22×10^6 cells per dish), as described earlier in this section. Cells were treated with 10^{-8} M $1,25(OH)_2D_3$ for 24 h. For immunoprecipitation, rat anti-VDR (MA1-710, Affinity Bioreagents, Golden, CO) was used, whereas an equal amount of rat IgG (IgG2b, CBL606, Chemicon, Billerica, MA) was used as a normalization control. For more detailed information on the ChIP assay, see Supplementary File 5.

Statistical analysis. For determination of relative quantitative gene expression, the corrected ΔCt method was used (Pfaffl, 2001). ΔCt-values were determined for each time point by subtracting the mean reference gene Ct-value at the time point of interest from the target gene Ct-value at the same time point: $\Delta Ct = Ct_{target} - Ct_{mean\ ref}$. Subsequently, all values were related to the T_0 time point by subtracting the ΔCt-value for T_0 from the ΔCt-value for T_x, the time point of interest: $\Delta Ct_{Tx} - \Delta Ct_{T0}$. For

each individual experiment, target gene expression per time point of interest (n-fold change) was determined separately. Afterwards, for each target gene, the mean n-fold changes and standard deviations in gene expression per time point of interest were calculated. In the silencing study, VDR knockdown percentages in the siRNA VDR-oligo cultures were determined by subtracting the VDR Ct-value from the mean reference gene Ct-value for each time point: $Ct_{ref} - Ct_{vdr}$. Subsequently, this value was subtracted from the value for the siRNA scrambled mock cultures or the value for the control cultures, to obtain ΔCt-values. VDR knockdown percentages were calculated using the formula: $100 \times 1-(1/E_{vdr}{}^{\Delta Ct})$.

Statistical analysis was performed using R Studio (version 0.96, http://www.rstudio.com) and R (version 2.15.2) (R Core Team, 2012). To determine whether the enrichment in the ChIP experiments was statistically significant, the data were examined for normal distribution, and a one-way ANOVA with Benjamini–Hochberg correction was used. For the rest of the data (target gene and PTHrP protein production), a mixed model for dependent data was used. This mixed model was optimized per target gene/protein and comparison. After it was determined whether the data were normally distributed, the random part of the model was determined (e.g., with random slopes and/or random intercepts). Thereafter, the fixed part of the model was optimized. Interaction of time and treatment (culture condition) appeared necessary in all cases. In the above mentioned tests, a *P*-value <0.05 was considered significant.

In vivo studies

Animals. The animal studies were approved by the institutional animal care committee (DEC 2008.III.03.024), as required by Dutch law. The colony of the transgenic Col2-pd2EGFP reporter mice was maintained at the SPF facilities with approval from the Dutch ministry of Infrastructure and Environment (DEM/SAS IG 99-057/03). The Col2-pd2EGFP transgenic mouse is appropriate for visualizing *Col2a1* expression, for monitoring chondrocyte differentiation, and for isolating murine growth plate chondrocytes by fluorescence activated cell sorting (FACS) (Tryfonidou et al., 2011).

Diets. Vitamin D_3 sufficient (control, TD 07370, 0.47% Ca, 0.3% P, 2,200 IU/kg vitamin D_3) and deficient (TD 89123, 0.47% Ca, 0.3% P, 0 IU/kg vitamin D_3) diets were purchased from Teklad Harlan SD (Indianapolis, IN). The vitamin D_3 content of these diets was re-analyzed by an independent laboratory (TNO Nutrition and Food Research, Zeist, The Netherlands); the vitamin D_3-sufficient diet contained 1,900 IU/kg and the vitamin D_3-deficient diet less than 20 IU/kg.

Experimental design. The mice were kept under standard conditions in the experimental animal facility of the University of Utrecht. Control offspring were obtained from dams maintained on the vitamin D_3-sufficient diet. Vitamin D_3-deficient pups were obtained by feeding the dams a vitamin D_3-deficient diet, from 2 weeks prior to mating until weaning. The weaned offspring were given the vitamin D_3-deficient diet until euthanasia at 6 weeks of age. In order to ensure vitamin D_3 deficiency, the pregnant females and their offspring were housed in filter-top cages, in which all fluorescent light was shielded, thereby preventing the endogenous production of vitamin D_3. Only those pups that had a weight within 2 SD of the mean at 3 weeks of age were included. The pups were weaned at approximately 3 weeks of age, depending on whether they could feed independently. Weaned pups were housed in groups according to diet and gender (in order to prevent mating): vitamin D_3 sufficient (VitD+), vitamin D_3 deficient (VitD−), and vitamin D_3 deficient supplemented with $1,25(OH)_2D_3$ (VitD−; +1,25D). The animals were weighed every week at fixed times. At 3 weeks of age, the vitamin D_3-deficient pups were given either 50 ng $1,25(OH)_2D_3$ (VitD−; +1,25D, intraperitoneal (IP), 1 ng/μl in sterilized peanut oil; mean dose 5 ng/g body weight, BW) or placebo (VitD−, sterilized peanut oil). Thereafter, the dose of vitamin D_3 metabolite was adjusted weekly, based on the mean BW of the respective group. The vitamin D_3-sufficient mice (VitD+) received placebo (sterilized peanut oil) IP. The IP administration was performed five times a week, lege artis, by the animal caretakers. At 6 weeks of age, blood (as much as possible) was obtained by cardiac puncture under general anesthesia, followed by cervical dislocation.

Serum biochemistry. Blood samples for the measurement of calcium (Ca), inorganic phosphate (P), and vitamin D_3 metabolites were collected in heparin-coated mini-collection-tubes (450479, Greiner Bio-One, Monroe, NC). For the measurement of PTH, blood was collected in EDTA-coated mini-collection tubes (REF 450475, Greiner Bio-One). Samples were immediately placed on ice until centrifugation and plasma was stored at −20°C until further analysis. Ca and P levels were measured according to standard procedures. Plasma $25(OH)D_3$ levels were measured to verify vitamin D_3 deficiency in the respective groups. $25(OH)D_3$ was extracted from 25 μl plasma with the Bligh and Dyer method (Bligh and Dyer, 1959) and quantified with the aid of a competitive binding assay. Thereafter, plasma samples for pairs of mice were pooled within the ascribed group (due to sample volume limitations) and vitamin D_3 metabolites were extracted from the pooled plasma using acetonitrile followed by a two-step phase extraction (C18 and Silicagel cartridge) and separated by straight phase HPLC. $25(OH)D_3$ was quantitatively determined using a competitive protein binding assay with a sensitivity of 2 nmol/L and $1,25(OH)_2D_3$ was quantitatively determined with a radioreceptor assay (Reinhardt et al., 1984), with a sensitivity of 40 pmol/L. Levels were corrected for procedural losses (recovery) with the aid of the specific 3H-labeled vitamin D_3 metabolite. PTH was determined according to the manufacturer's instructions (intact PTH mouse EIA, Alpco Diagnostics, Salem, NH).

Growth plate histology. After euthanasia, the right tibia was removed and fixed in 4% formaldehyde (pH = 7.4, 4°C) for 24 h and decalcified in 0.5 M EDTA in Ca–Mg free Hanks solution (pH = 7.8, 4°C) for 7 days. After demineralization, the bones were washed and bisected in the sagittal plane. One half was embedded in Tissue Tek (O.C.T. compound, Sakura Fine Technical Co. Ltd., Tokyo, Japan) and stored at −70°C until further processing. The other half of the tibia was embedded in paraffin and stored at 4°C until further processing.

Quantitative determination of the expression of target genes. From each mouse, growth plate chondrocytes were isolated as described previously (Tryfonidou et al., 2011). Briefly, after euthanasia, the long bones and rib cartilage (except for the right tibia) were removed and submerged in cold (4°C) Hanks + 2% pen/strep. The growth plate and adjacent tissue from each animal was dissected with the aid of a stereoscope and scalpel blade, pooled, and digested overnight at 37°C 5% CO_2 with collagenase II (4176, Worthington, Lakewood, NJ). After digestion, cells were suspended in DMEM/F12 + glutamine without phenol red (21041, Gibco, Bleiswijk, The Netherlands) with 10% FCS (PAA) and 2% pen/strep. The cell solution was individually run through a FACS (BD Influx cell sorter, BD Biosciences) with a nozzle of 100 μm. After collection, the cells were lysed in 350 μl RLT buffer (Qiagen) containing 1% β-mercaptoethanol and stored at −70°C until further processing. RNA isolation, cDNA production, and RT-qPCR were performed as described for the in vitro studies. The relative level of gene expression of *Pthrp*, *Pthr1*, *Vdr*, and *ColX* was determined (Supplementary File 2).

Immunofluorescent staining. Immunofluorescent staining of bone for collagen type X was performed as described previously (Tryfonidou et al., 2011) on 10-μm cryosections, in order to define the pattern of GFP expression in relation to the phase of differentiation of growth plate chondrocytes. Briefly, after sections were rinsed with PBS, antigen retrieval with 4 mg/ml bovine hyaluronidase (450 IU/mg, Sigma-Aldrich, St. Louis, MO) was

performed. After blockade of aspecific binding sites with 10% goat serum, sections were incubated with rabbit polyclonal anti-mouse collagen type X (PXNC2, 1:100) overnight at 4°C (Lunstrum et al., 1999). Goat anti-rabbit ALEXA 568 (1:100, Invitrogen) was used as second antibody. Nuclear counterstaining was performed with TO-PRO®-3, and the slides were mounted in Prolong Gold anti-fade reagent (Invitrogen). Confocal microscopy was performed using a Leica TCS SP confocal laser scanning microscope. Immunofluorescent staining images were prepared using Adobe Photoshop CS5.1. Linear adjustment of brightness, contrast, and color balance was applied to every pixel in the image.

Immunohistochemistry. Paraffin sections of 4 μm were cut and mounted on Microscope KP plus slides (Klinipath B.V., Duiven, The Netherlands). Each slide contained three sections: one section of each group in an ad random order. Slides were deparaffinized through xylene (two times 5 min) and graded ethanol (96%, 80%, 70%, 60%, 30%; 5 min each), followed by two rinses with PBS. Mid-sagittal sections of the three samples representing each group were included in the same Pap-pen circle and were thus incubated under identical conditions. Thereafter, antigen retrieval was performed (Supplementary File 3). After inhibition of endogenous peroxidase for 5 min, sections were preincubated with blocking buffer for 30 min at room temperature (RT). The sections were incubated overnight with first antibody at 4°C. For further processing, depending on the first antibody, either the EnVision™-HRP detection system (Dako), the goat ImmunnoCruz™ system (sc-2053, Santa Cruz Biotechnology, Inc., Heidelberg, Germany), or specific second antibody was applied for 30 min at RT, followed by incubation with streptavidin-conjugated with HRP for 30 min at RT. All antibodies were visualized with the liquid DAB+ substrate chromogen system (K3468, Dako, Glostrup, Denmark). In control experiments, the first antibody was omitted and, depending on the antibody, either substitution of the first antibody with its respective serum, and/or competition of the first antibody with corresponding peptides available for PTHR1 (sc-12777 P) was performed. Raw images were made using a Colorview IIIU digital camera (Olympus, Zoeterwoude, The Netherlands) mounted to a BX-40 microscope (Olympus). Histomorphometry was performed on the raw images with Image J software package (Rasband NIH, Bethesda, ML). The mean width of the growth plate (GPl.Th.) was calculated from the width of the growth plate at 20 set locations. The mean width of the proliferative ($GPl.Th._{Pr}$) and hypertrophic zone ($GPl.Th._{Hp}$) was determined in a similar way. The proliferative zone comprised the region containing columnar chondrocytes of constant size, whereas the hypertrophic zone was defined by collagen type X staining.

A custom-made color range selection optimized for each immunohistochemical stain was used to determine the area within the growth plate that stained positive. For each growth plate section, the proportion of the surface area of the growth plate that stained positively for the respective protein was calculated, as were the mean gray value and integrated density. Quantitative image analysis of the nuclear VDR area that stained positive was performed using the Image J plugin ImmunoRatio, which calculates the percentage of positively stained nuclear area (labeling index) by using a color deconvolution algorithm for separating the staining components (diaminobenzidine and hematoxylin) and adaptive thresholding for nuclear area segmentation.

In vitro studies with primary growth plate chondrocytes

Cell culture and experimental design. The isolation of primary growth plate chondrocytes from the limbs of three 9-day-old Col2-pd2EGFP mice was performed as described previously (Tryfonidou et al., 2011). Approximately 26% of the selected population was positive for GFP. On differentiation day 0 (T_0), droplets of 10 μl (containing approximately 20,000 cells) were placed on a Falcon Primaria petri dish (353803, BD Biosciences), not touching each other to create multiple high-density micro-cultures. After 2 h, 10 ml differentiation medium was added as describe previously, and after 2 days (T_2), 10^{-8} M $1,25(OH)_2D_3$ (Dishman BV, Veenendaal, The Netherlands) was daily added to the $1,25(OH)_2D_3$-treated cultures. In a similar manner, high-density microcultures on chamber slides (Lab-Tek®) were studied from differentiation day 0 until day 7. At the time points T_0, T_3, T_5, and T_7 (the digits indicate the number of days after differentiation culture medium was first added to the wells), medium for PTHrP ELISA and cells for RNA isolation were obtained, and formalin-fixed slices were stained for collagen type X (as described previously). Confocal microscopy was performed using a Leica SPEII confocal laser-scanning microscope (Leica Microsystems, Wetzlar, Germany). The concentration of PTHrP in culture media was measured with an ELISA (ELISA kit for mouse PLP, USCN E90819Mu), according to the manufacturer's instructions.

Chromatin immunoprecipitation (ChIP) assay. The ChIP analysis of the cultured primary growth plate chondrocytes (Falcon Primaria petri dish) was performed as described for the in vitro studies.

Quantitative determination of the expression of target genes. RNA isolation, cDNA production, and RT-qPCR were performed as described for the in vitro studies. Ultimately, the relative gene expression of *Pthrp*, *Pthr1*, *Vdr*, and *ColX* was determined (Supplementary File 2).

Statistical analysis. After it was determined that the data had a normal distribution, a one-way ANOVA with Benjamini–Hochberg correction was used to analyze the significance of differences in the mean (±SD) width of the growth plate (including the proliferative and hypertrophic zone), plasma parameters, target gene expression, and ChIP assay results between the different groups. For body weight and PTHrP protein levels, a mixed model for dependent data was used as described at the in vitro studies. In the above-mentioned tests, a P-value <0.05 was considered significant.

Results

In vitro studies with the ATDC5 cell line

The effect of PTHrP on the vitamin D_3 pathway. Protein and mRNA expression of 1α- and 24-hydroxylase was stable during culture and appeared not affected by treatment with 10^{-8} M PTHrP (data not shown). At all time points, *Vdr* gene expression was significantly higher in the PTHrP-treated cultures than in the control cultures ($P < 0.01$, Fig. 1A). After the first addition of PTHrP at T_0, *Vdr* gene expression increased significantly to reach a maximum at T_4 and declined thereafter. At T_{28}, 4 h after the second addition of PTHrP, *Vdr* gene expression was significantly higher than that at T_{24} ($P < 0.01$), but significantly lower than that at T_4 ($P < 0.001$). *Vdr* gene expression did not change substantially after T_{28}. VDR protein levels were also significantly higher at time points T_{24} and T_{48} in the PTHrP-treated cultures than in the control cultures ($P < 0.01$, Fig. 1B). Altogether, these data indicate that PTHrP treatment increased ATDC5 chondrocyte sensitivity for $1,25(OH)_2D_3$ by upregulating VDR expression and not by influencing 1α- and/or 24-hydroxylase expression.

The effect of vitamin D_3 on the PTHrP pathway. Treatment of ATDC5 chondrocytes with 10^{-8} M $1,25(OH)_2D_3$ increased the activity of the vitamin D_3 pathway (Armbrecht and Boltz, 1991), as evidenced by a more than 1,000 times increased expression of the *24-OHase* gene compared with control cultures (data not shown). 10^{-8} M $1,25(OH)_2D_3$ treatment also significantly increased VDR gene and protein expression in ATDC5 chondrocytes in the prehypertrophic phase of differentiation ($P < 0.05$, Fig. 1A,B) (Davoodi et al., 1995; Klaus et al., 1998; Healy et al., 2005a). *Pthrp* gene expression was significantly higher in the 10^{-8} M $1,25(OH)_2D_3$-treated cultures than in the control cultures at all time points ($P < 0.001$, Fig. 1C). In contrast, the PTHrP protein content of

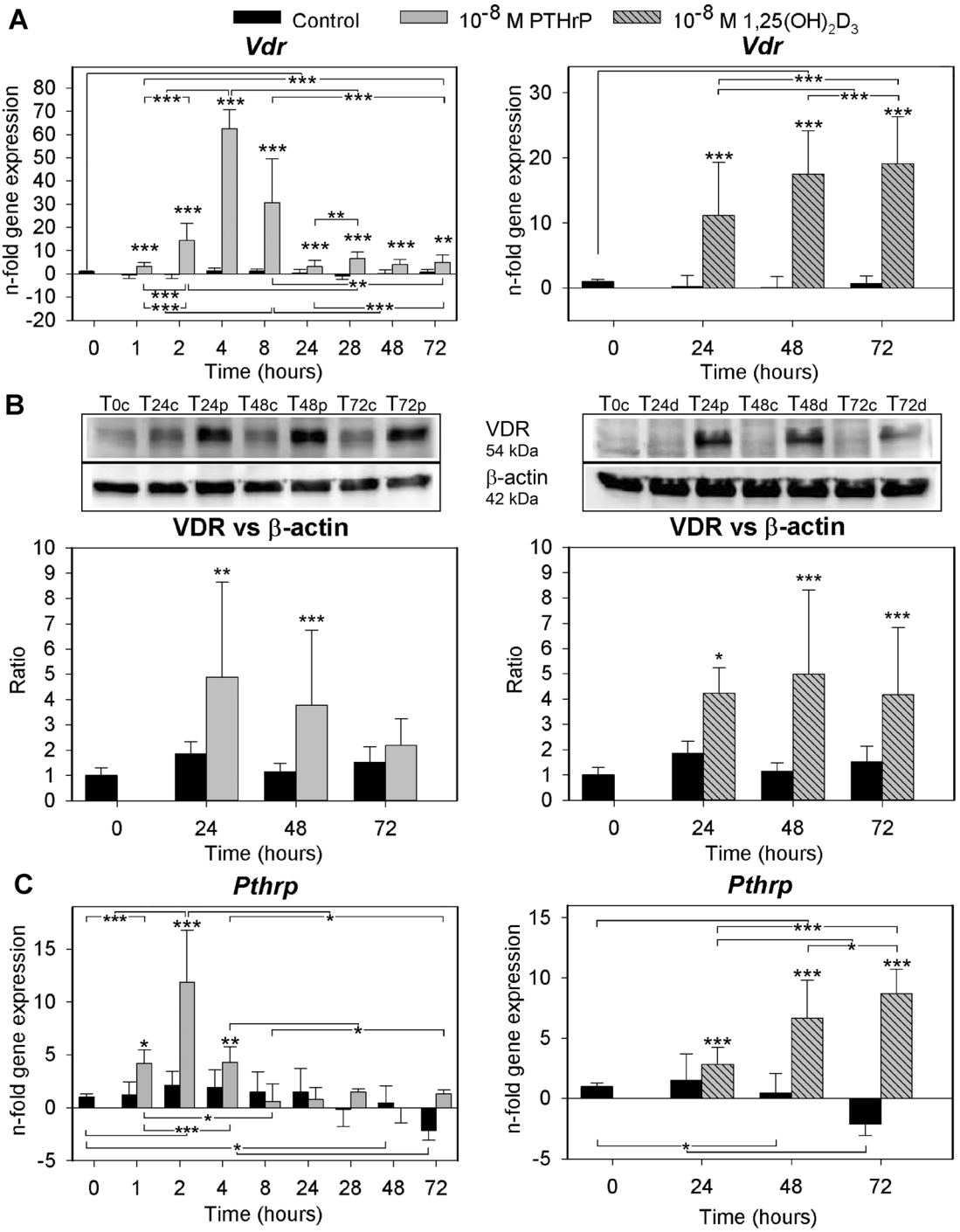

D

PTHrP protein levels of culture medium corrected for DNA content				
	T_0	T_{24}	T_{48}	T_{72}
Control	55.0±13.5	43.0±2.7	128.7±6.1	140.8±23.1
10^{-8} M 1,25(OH)$_2$D$_3$		27.3±6.1	20.3±2.0***	14.7±3.7***

Fig. 1. VDR and PTHrP expression in 1,25(OH)$_2$D$_3$- and PTHrP-treated ATDC5 chondrocytes in the prehypertrophic phase of differentiation. ATDC5 cells were treated starting from day 7 of differentiation (T_0) with 10^{-8} M PTHrP or 1,25(OH)$_2$D$_3$ at T_0, T_{24}, and T_{48}. A. Relative *Vdr* gene expression (mean ± SD; n = 8). T_0 in the control culture was set at 1. B: VDR protein expression expressed as VDR/β-actin ratio (mean ± SD; n = 6). T_0 in the control culture was set at 1. c = control culture, *P* = 10^{-8} M PTHrP-treated culture, d = 10^{-8} M 1,25 (OH)$_2$D$_3$-treated culture. C: Relative *Pthrp* gene expression (mean ± SD; n = 8). T_0 in the control culture was set at 1. D: PTHrP protein levels corrected for DNA content (pg PTHrP/ng DNA) in ATDC5 culture media of control cultures and 10^{-8} M 1,25(OH)$_2$D$_3$-treated cultures, determined using a PTHrP ELISA (mean ± SD; n = 4). *$P < 0.05$, **$P < 0.01$, ***$P < 0.001$.

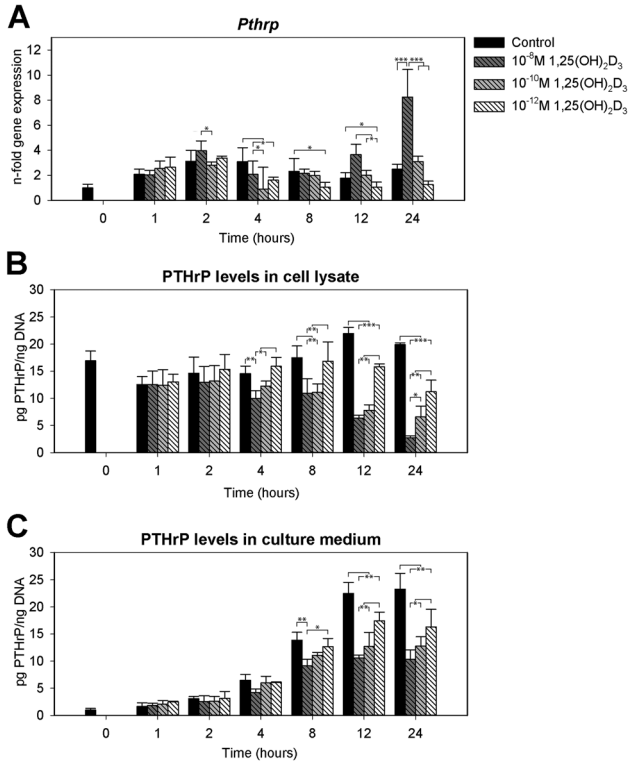

Fig. 2. ***Pthrp*** **mRNA superinduction phenomenon. 10^{-8}, 10^{-10}, and 10^{-12} M $1,25(OH)_2D_3$-treated ATDC5 cell cultures were compared with control cultures. At T_0 (on day 7 of differentiation, i.e., the prehypertrophic phase of the ATDC5 chondrocytes), $1,25(OH)_2D_3$ was added to the culture medium and the respective PTHrP gene (A) and protein content of cell lysates (B) and culture media (C) were determined at T_{1-24} after $1,25(OH)_2D_3$ treatment (mean ± SD; n = 6 for control and 10^{-8} M $1,25(OH)_2D_3$ cultures and n = 4 for 10^{-10} and 10^{-12} M $1,25(OH)_2D_3$ cultures). Relative** ***Pthrp*** **gene expression at T_0 in the control culture was set at 1. The pharmacological "*Pthrp* mRNA superinduction" phenomenon is only observed in the 10^{-8} M $1,25(OH)_2D_3$-treated ATDC5 chondrocytes, and can be avoided with lower physiological regimes. *$P < 0.05$, **$P < 0.01$, ***$P < 0.001$.**

the medium from $1,25(OH)_2D_3$-treated cultures was significantly lower than that of medium from the control cultures at T_{48} and T_{72} ($P < 0.001$, Fig. 1D). This seemingly contradictory result could be attributed to a phenomenon called "mRNA superinduction." It has been reported that the inhibition of PTHrP protein synthesis leads to the induction of *Pthrp* mRNA expression ("mRNA superinduction") in a number of cell lines (Ikeda et al., 1990). We explored this possibility in the ATDC5 cell line by measuring PTHrP mRNA and protein levels (in culture medium and cell lysate, corrected for DNA content) in the first 24 h after treatment with $1,25(OH)_2D_3$. PTHrP protein production decreased by 10^{-8} M $1,25(OH)_2D_3$ treatment from T_4/T_8 onward ($P < 0.01$, Fig. 2B,C) and remained lower in the 10^{-8} M $1,25(OH)_2D_3$-treated cultures than in the control cultures until T_{72} (Fig. 1D). In contrast, *Pthrp* mRNA expression significantly increased from T_{24} onward by 10^{-8} M $1,25(OH)_2D_3$ treatment (Figs. 1A and 2C). Given the time line of these events, where the increase in *Pthrp* mRNA expression (T_{24}) is preceded by an initial significant decrease in PTHrP protein production (T_4/T_8), it seems reasonable to assume that the increased *Pthrp* mRNA levels were due to the "mRNA superinduction" phenomenon. To determine whether this observed effect was physiological or pharmacological, we conducted an additional experiment investigating the time line of PTHrP mRNA and protein expression in the presence of 10^{-8}, 10^{-10}, and 10^{-12} M $1,25(OH)_2D_3$. PTHrP protein levels were dose-dependently influenced by $1,25(OH)_2D_3$ treatment (Fig. 2B,C). Moreover, the increased *Pthrp* mRNA expression observed in the 10^{-8} M $1,25(OH)_2D_3$-treated ATDCs chondrocytes (at T_{24}), was not observed in the 10^{-10} and 10^{-12} M $1,25(OH)_2D_3$-treated cells. This indicates that the "*Pthrp* mRNA superinduction" phenomenon, only observed in the 10^{-8} M $1,25(OH)_2D_3$-treated ATDC5 chondrocytes, is pharmacological and can be avoided with lower physiological $1,25(OH)_2D_3$ regimes.

Functional binding of $1,25(OH)_2D_3$ to the promoter region of the PTHrP gene. Computational analysis of the PTHrP promoter revealed the presence of two VDR binding elements (Fig. 3A). ChIP experiments showed a significant 2-fold enrichment of VDRE1 ($P < 0.01$) and a 1.6-fold enrichment of VDRE2 (n.s.) in the PTHrP promoter (Fig. 3B). No enrichment was observed in the PTHrP negative control (sequence 1,000 bp upstream of VDRE2) and a significant 2.5-fold enrichment was observed in the positive control (24-hydroxylase promoter, $P < 0.05$, Fig. 3B). Altogether, this indicates that in ATDC5 chondrocytes in the prehypertrophic phase of differentiation, $1,25(OH)_2D_3$ binds to its nuclear receptor, the VDR, and together they bind to a $1,25(OH)_2D_3$-responsive region (VDRE1) in the PTHrP promoter. In this way, $1,25(OH)_2D_3$ directly regulates *Pthrp* expression via genomic effects.

Computational analysis of the PTHR1 promoter revealed the presence of two VDREs (Fig. 3C). ChIP experiments showed a 1.4-fold enrichment of both VDRE1 and VDRE2, and a 2.1-fold enrichment of the VDRE combination (region containing both the expected VDRE1 and VDRE2) in the PTHR1 promoter (Fig. 3D). However, these results were not significant and the PTHR1 negative control (sequence 1,000 bp upstream of the expected VDREs) also revealed a 1.5-fold enrichment of the VDR antibody. Altogether, this indicates that there is no functional binding of $1,25(OH)_2D_3$ and the VDR to a VDRE in the PTHR1 promoter of ATDC5 chondrocytes in the prehypertrophic phase of differentiation.

Determination of the role of the VDR in the paracrine feedback loop between PTHrP and $1,25(OH)_2D_3$. To clarify the role of the VDR in the paracrine feedback loop between PTHrP and $1,25(OH)_2D_3$, we successfully silenced the VDR in 100% confluent ATDC5 chondrocytes in the prehypertrophic phase of differentiation; significant VDR knockdown was seen at all time points in the control + VDR-oligo cultures and the $1,25(OH)_2D_3$ + VDR-oligo cultures ($P < 0.05$, Fig. 4A,C).

Up- and downregulated PTHrP protein production in the scrambled mock cultures compared with the control cultures was observed at several time points (both with and without $1,25(OH)_2D_3$ supplementation, Fig. 4D), which can be explained by off-target effects of the scrambled mock siRNA sequence (Persengiev et al., 2004). The culture medium PTHrP protein content increased over time in the control cultures, whereas it decreased over time in the $1,25(OH)_2D_3$-treated cultures, with the difference being significant at T_{24}–T_{72} ($P < 0.05$, Fig. 4D). At T_{48} and T_{72}, PTHrP protein levels in the $1,25(OH)_2D_3$ + VDR-oligo cultures were significantly higher than in the $1,25(OH)_2D_3$ cultures ($P < 0.05$), indicating that VDR silencing counteracted the $1,25(OH)_2D_3$-mediated inhibitory effect on PTHrP protein production in ATDC5 chondrocytes in the prehypertrophic phase of differentiation.

The role of the paracrine PTHrP-$1,25(OH)_2D_3$ feedback loop in hypertrophic chondrocyte differentiation. $1,25(OH)_2D_3$ treatment of the prehypertrophic ATDC5 cultures decreased the DNA content by about 40% whereas

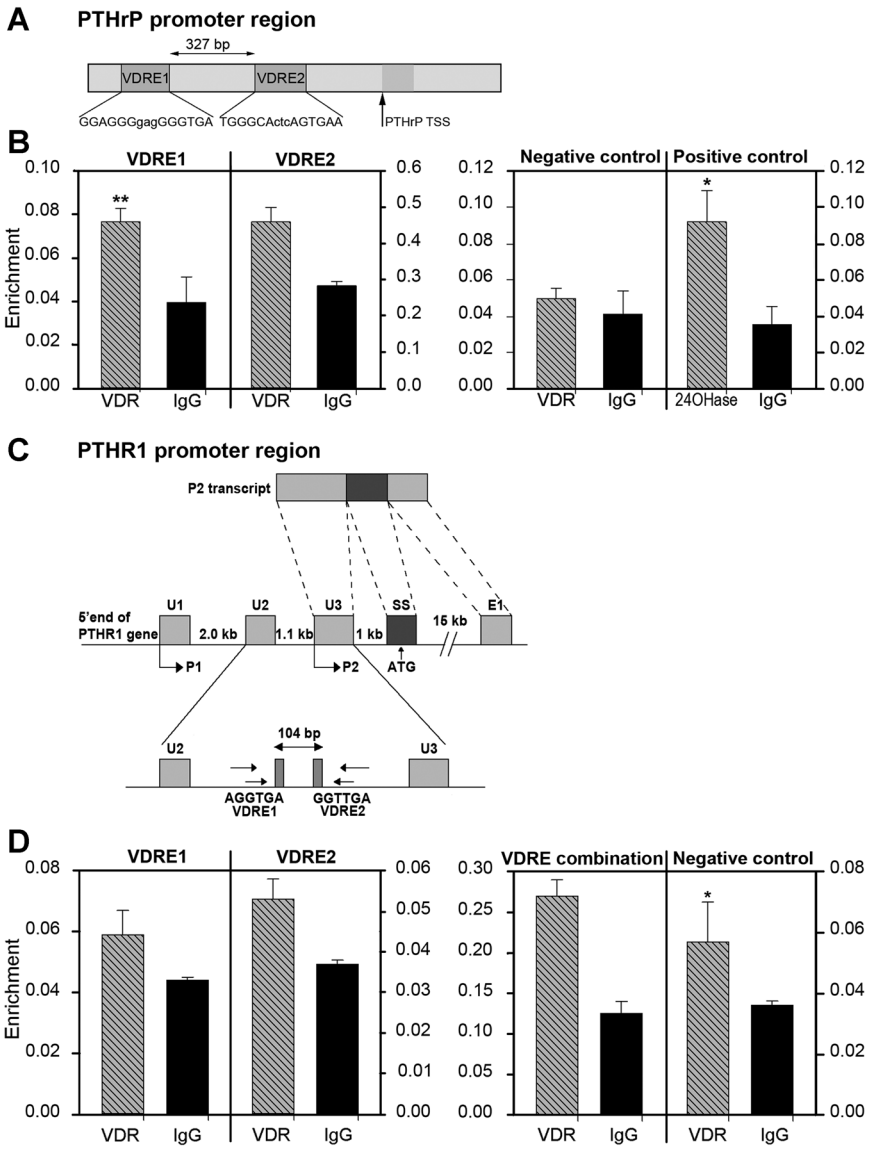

Fig. 3. Identification of a functional vitamin D_3 response element (VDRE) in the PTHrP and PTHR1 promoter region. A: Schematic presentation of the mouse PTHrP promoter region with location of the vitamin D_3 response elements (VDREs). Primers were designed for VDRE1 and VDRE2. The location of VDRE1 and VDRE2 upstream from TSS is 913 and 571 bp, respectively. bp, base pairs; TSS, transcription start site. B: VDR ChIP assay performed on ATDC5 cells in the prehypertrophic phase of differentiation. Cells were fixed after 24 h of treatment with 10^{-8} M $1,25(OH)_2D_3$. IgG was used as normalization control and a sequence 1,000 bp upstream of VDRE2 was used as a negative control. Enrichment is given as mean ± SD; n = 8. The results indicate functional binding of $1,25(OH)_2D_3$ and its receptor, the VDR, to the PTHrP promoter region. C: Overview of expected VDREs in the PTHR1 promoter region. The PTHR1 gene has two promoter regions, P1 and P2. In bone and cartilage, the P2 promoter controls PTHR1 expression, whereas expression of P1 is restricted mainly to the kidney. The location of the expected VDRE1 (AGGTGA) and VDRE2 (GGTTGA) is 2,092; and 2,027 bp upstream from TSS, respectively. The arrows indicate the position of the primers used in this study. bp, base pairs; TSS, transcription start site. D: VDR ChIP assay performed on ATDC5 cells in the prehypertrophic phase of differentiation. The VDRE combination contains both the expected VDRE1 and VDRE2 sequence. The same conditions apply as described with B. *$P < 0.05$, **$P < 0.01$.

the addition of PTHrP increased the DNA content by about 30% compared with the control cultures (data not shown). Gene expression of the (pre) hypertrophic differentiation markers *Col9*, *Pthr1*, and *ColX* increased significantly over time in the control cultures ($P < 0.05$), but not in the PTHrP- and $1,25(OH)_2D_3$-treated cultures (Fig. 5A). Generally, *Pthr1*, *Col9*, and *ColX* gene expression was higher in the control cultures than in the PTHrP- or $1,25(OH)_2D_3$-treated cultures at all time points. However, Western blot analysis indicated that only on differentiation day 14 (T_{168}), collagen type X protein expression was significantly lower in the PTHrP- and 1,25 $(OH)_2D_3$-treated cultures than in the control cultures ($P < 0.001$, Fig. 5B), but not on differentiation day 10 (T_{72}). This indicates that both $1,25(OH)_2D_3$ and PTHrP treatment inhibited hypertrophic differentiation of the ATDC5 chondrocytes, which was noticed earlier at the mRNA than at the protein level.

To clarify the role of the paracrine feedback loop between PTHrP and $1,25(OH)_2D_3$ in growth plate chondrocyte differentiation, we silenced the VDR in ATDC5 chondrocytes in the prehypertrophic phase of differentiation. In the control + scrambled mock and the control + VDR-oligo

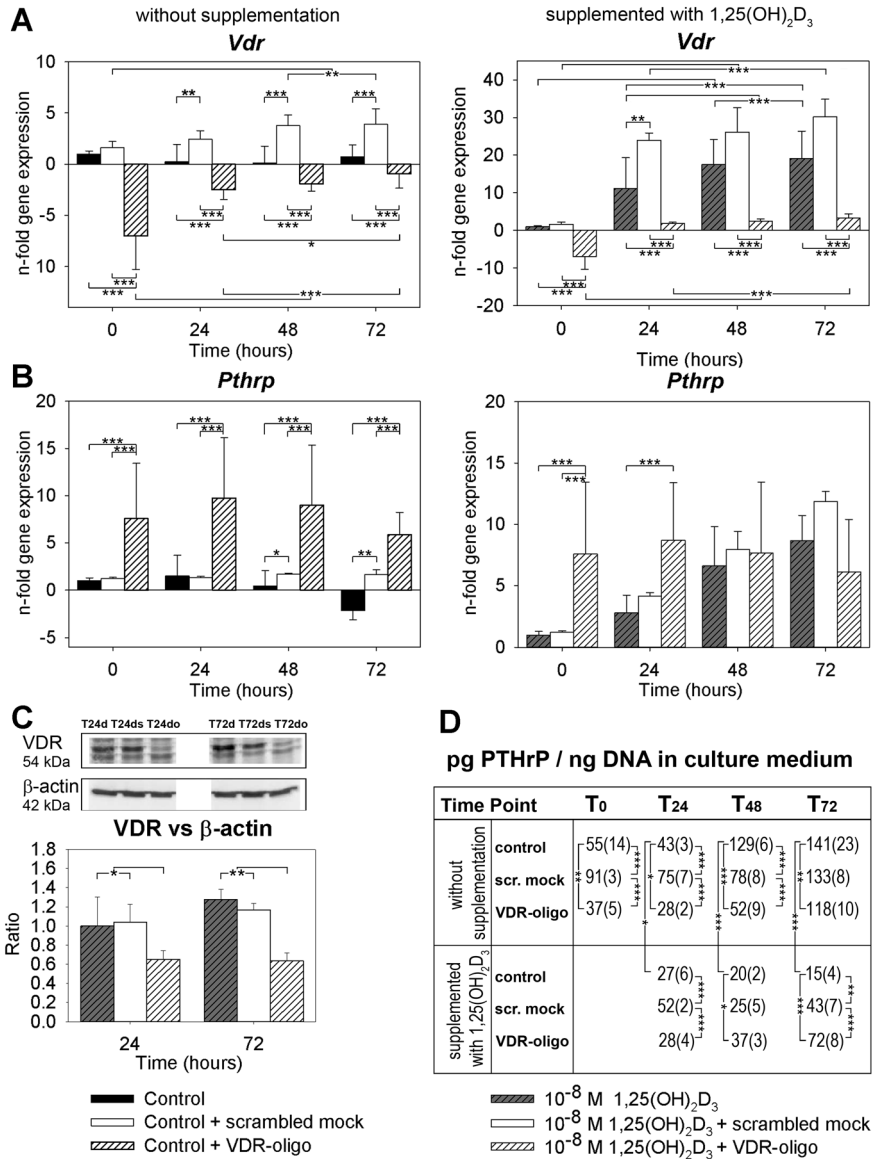

Fig. 4. The role of VDR in the paracrine feedback loop between PTHrP and 1,25(OH)$_2$D$_3$. A,B: Relative *Vdr* and *Pthrp* gene expression in ATDC5 cells in the prehypertrophic phase of differentiation (mean ± SD; n = 6). In the VDR-oligo groups, silencing of the VDR was performed on differentiation day 4. At T_0 (day 7 of differentiation), T_{24}, and T_{48}, 10^{-8} M 1,25(OH)$_2$D$_3$ was added to the three 1,25(OH)$_2$D$_3$-treated culture groups. Relative target gene expression at T_0 in the control culture was set at 1. C: Western blot analysis confirming the successful siRNA transfection in 10^{-8} M 1,25(OH)$_2$D$_3$-treated prehypertrophic ATDC5 cells with approximately 50% downregulation of VDR production. Time is shown in hours after 1,25(OH)$_2$D$_3$ was first added and the VDR/β-actin ratio (mean ± SD; n = 3) in the 1,25(OH)$_2$D$_3$ culture at T_{24} was set at 1. d = 10^{-8} M 1,25(OH)$_2$D$_3$-supplemented culture, ds = 1,25(OH)$_2$D$_3$ + scrambled mock culture, do = 1,25(OH)$_2$D$_3$ + VDR-oligo culture. D: PTHrP protein levels (mean ± SD; n = 3) corrected for DNA content in ATDC5 culture media, determined using a PTHrP ELISA. *$P < 0.05$, **$P < 0.01$, ***$P < 0.001$.

cultures, *ColX* gene expression did not increase over time, in contrast to what was observed in the control cultures (Fig. 6A). For the PTHrP- and 1,25(OH)$_2$D$_3$-treated ATDC5 cultures, no significant differences in collagen type X expression between the non-silenced (PTHrP/1,25(OH)$_2$D$_3$) and the VDR silenced (PTHrP/1,25(OH)$_2$D$_3$ + VDR-oligo) cultures were observed (Fig. 6A,B), indicating that VDR silencing did not counteract the PTHrP/1,25(OH)$_2$D$_3$-mediated inhibitory effect on collagen type X gene and protein expression in ATDC5 chondrocytes in the prehypertrophic phase of differentiation. In contrast, *Pthr1* expression was significantly upregulated in the 1,25(OH)$_2$D$_3$ + VDR-oligo cultures at T_{48} and T_{72} ($P < 0.01$, Fig. 6), indicating that VDR silencing counteracted the 1,25(OH)$_2$D$_3$-mediated inhibitory effect on *Pthr1* expression in ATDC5 chondrocytes in the prehypertrophic phase of differentiation.

Generally, *ColX* and *Vdr* gene expression was significantly higher in the scrambled mock cultures than in the non-silenced control cultures, whereas the scrambled mock treatment did not affect *Pthr1* and *Pthrp* expression (Figs. 4A,B and 6A). The difference in *ColX* and *Vdr* gene expression was, however, not

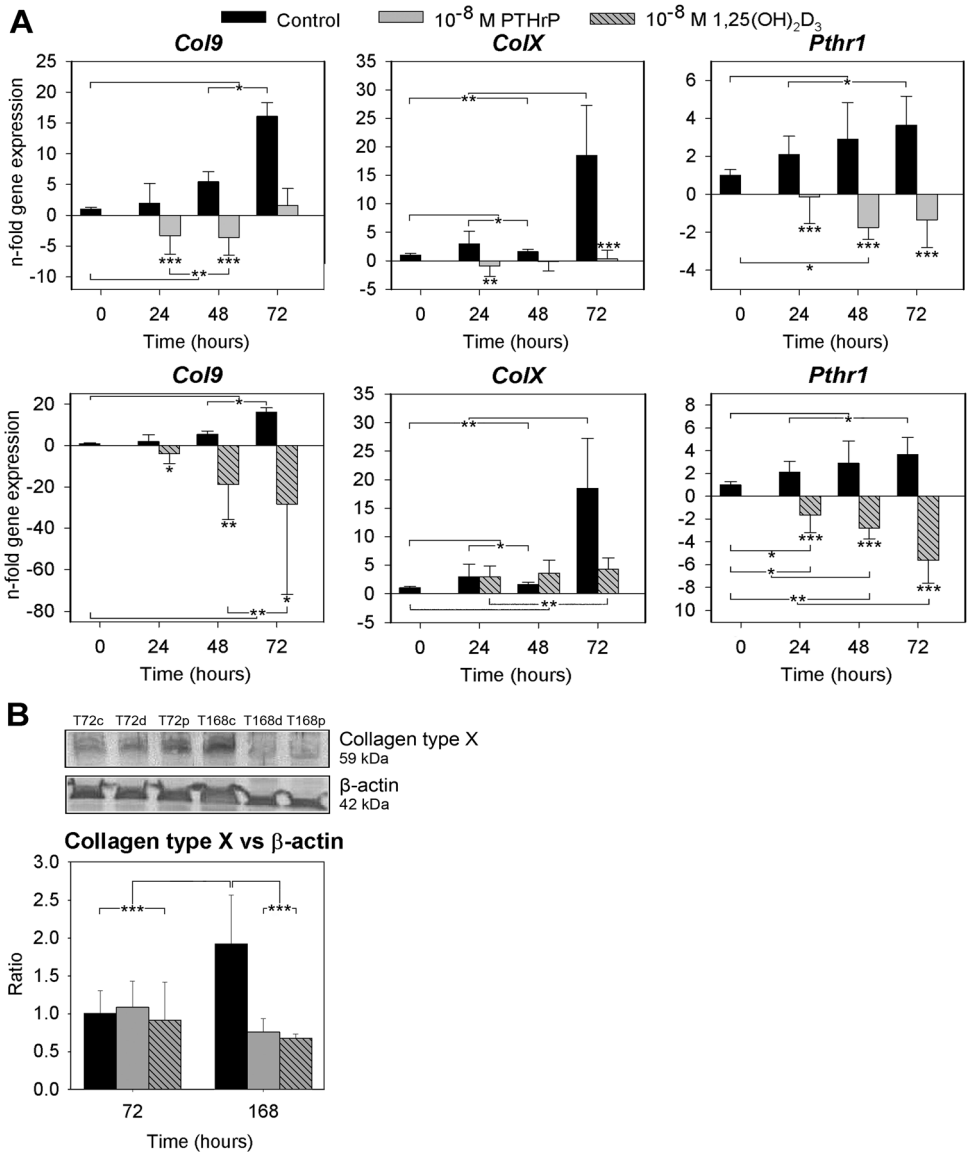

Fig. 5. The role of the paracrine PTHrP-1,25(OH)$_2$D$_3$ feedback loop in hypertrophic chondrocyte differentiation. A: Relative *Col9*, *ColX*, and *Pthr1* gene expression in PTHrP- or 1,25(OH)$_2$D$_3$-treated ATDC5 cell cultures compared with control cultures (mean ± SD; n = 8). 10^{-8} M PTHrP or 1,25(OH)$_2$D$_3$ was added daily from T$_0$, which was day 7 of differentiation, that is, the prehypertrophic phase of the ATDC5 chondrocytes. Relative target gene expression at T$_0$ in the control culture was set at 1. B: Collagen type X protein expression expressed as Collagen type X/β-actin ratio (mean ± SD; n = 3). Time is shown in hours after PTHrP/1,25(OH)$_2$D$_3$ was first added to the culture medium on differentiation day 7. T$_{72}$ in the control culture was set at 1. c = control culture, P = 10^{-8} M PTHrP-treated culture, d = 10^{-8} M 1,25(OH)$_2$D$_3$-treated culture. *P < 0.05, **P < 0.01, ***P < 0.001.

accompanied with differences in VDR and collagen type X protein expression between the scrambled mock and the non-silenced control cultures (Figs. 4C and 6B), indicating that the scrambled mock-induced upregulated mRNA expression was not translated into increased protein expression. Most probably, the upregulated *ColX* and *Vdr* mRNA expression can be attributed to off-target effects of the scrambled mock sequence (Persengiev et al., 2004).

In vivo studies

Animals and biochemistry. From 4 weeks of age onward, the control vitamin D$_3$-sufficient (VitD+) mice weighed significantly more than the VitD− mice ($P < 0.001$, Supplementary file 6A). Plasma 25(OH)D$_3$ levels confirmed vitamin D$_3$ deficiency in VitD− mice ($P < 0.001$, Supplementary file 6A). As expected, the plasma concentration of 1,25(OH)$_2$D$_3$ was significantly higher in VitD−; +1,25D mice than in VitD+ and VitD− mice ($P < 0.01$). Plasma calcium (Ca) levels were significantly lower in VitD− mice than in VitD+ mice ($P < 0.01$), but were significantly higher in VitD−; +1,25D mice than in VitD− and VitD+ mice ($P < 0.01$). Inorganic phosphate (P) plasma levels were not significantly different between groups, but PTH levels were significantly higher in VitD− mice than in VitD+ and VitD−; +1,25D mice ($P < 0.001$).

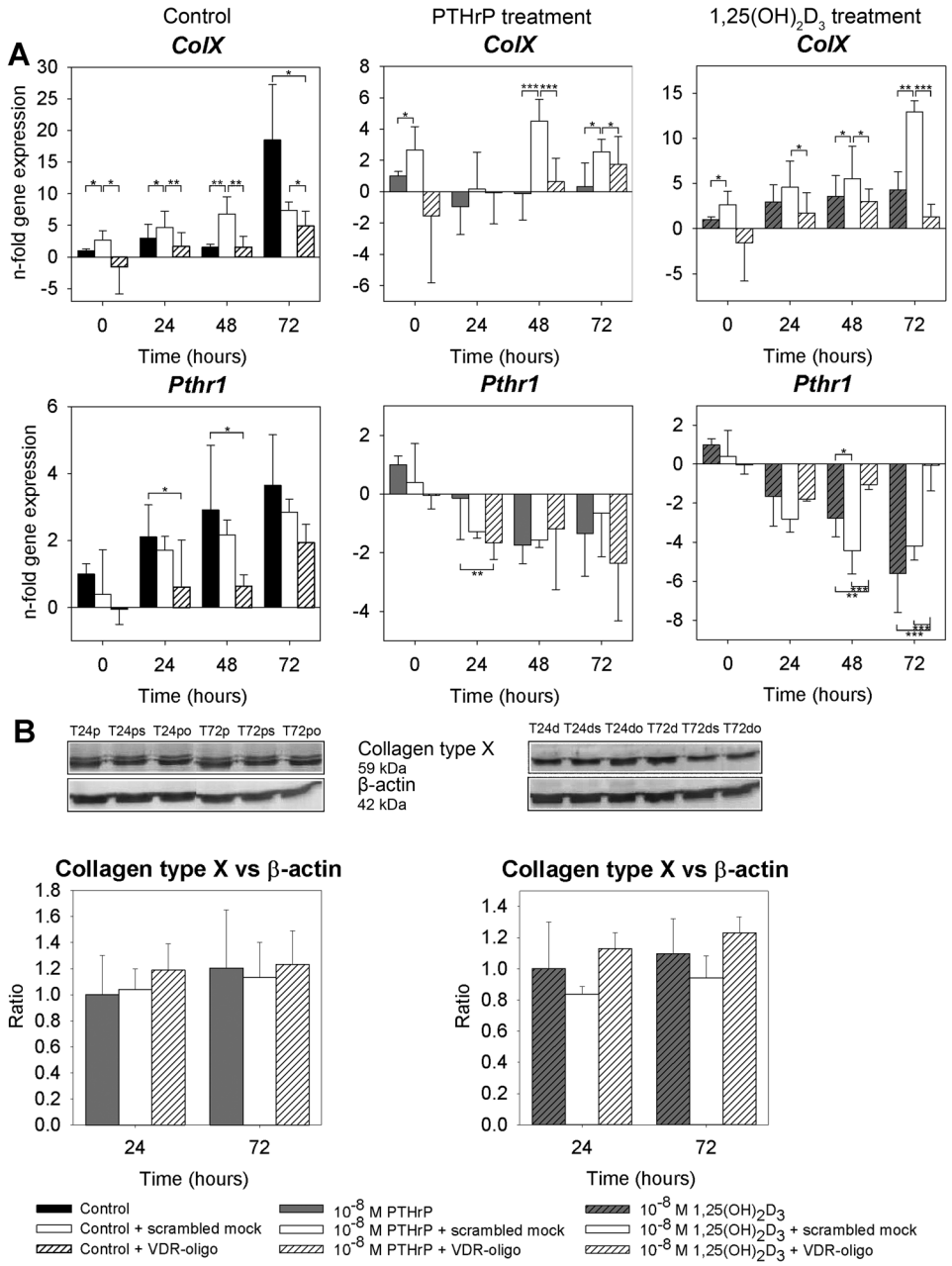

Fig. 6. The role of the VDR in the paracrine PTHrP-1,25(OH)$_2$D$_3$ feedback loop during hypertrophic chondrocyte differentiation. A: Relative *ColX* and *Pthr1* gene expression corrected for reference genes in ATDC5 cells in the prehypertrophic differentiation phase (mean ± SD; n = 6). In the VDR-oligo groups, silencing of the VDR was performed on differentiation day 4. 10^{-8} M PTHrP or 1,25(OH)$_2$D$_3$ was added daily, starting at T_0, which was day 7 of differentiation. Relative target gene expression at T_0 in the control culture was set at 1. B: Collagen type X protein expression in 10^{-8} M PTHrP- and 1,25(OH)$_2$D$_3$-treated ATDC5 cells silenced for the VDR. Time is shown in hours after PTHrP/1,25(OH)$_2$D$_3$ was first added to the culture medium on differentiation day 7. The collagen type X/β-actin ratio (mean ± SD; n = 3) in the PTHrP/1,25 (OH)$_2$D$_3$ culture at T_{24} was set at 1. p = PTHrP culture, pm = PTHrP + scrambled mock culture, po = PTHrP + VDR-oligo culture, d = 1,25 (OH)$_2$D$_3$ culture, dm = 1,25(OH)$_2$D$_3$ + scrambled mock culture, do = 1,25(OH)$_2$D$_3$ + VDR-oligo culture. *$P < 0.05$, **$P < 0.01$, ***$P < 0.001$.

Growth plate histomorphometry. The mean growth plate height (GPl.Th) was significantly higher in VitD− mice than in VitD+ and VitD−; +1,25D mice ($P < 0.001$, Fig. 7A). The mean GPl.Th.$_{Pr}$ did not differ between groups, whereas the GPl.Th.$_{Pz}$/GPl.Th ratio was significantly lower in VitD− mice than in the other groups ($P < 0.05$). The mean GPl.Th.$_{Hyp}$ and the ratio of GPl.Th.$_{Hyp}$/GPl.Th were significantly higher in VitD− mice than in VitD+ or VitD−; +1,25D mice ($P < 0.05$). The standard deviation of GPl.Th.$_{Hyp}$, a measure of the irregularity of the hypertrophic zone, was also significantly higher in VitD− mice than in VitD+ and VitD−; +1,25D mice ($P < 0.01$, Fig. 7A). The Col2-pd2EGFP vitamin D_3-deficient mice thus showed the classical signs of low body weight, hypocalcemia, hyperparathyroidism, and rickets with an enlarged growth plate. The latter was mainly due to an increased and irregular hypertrophic zone (Donohue and

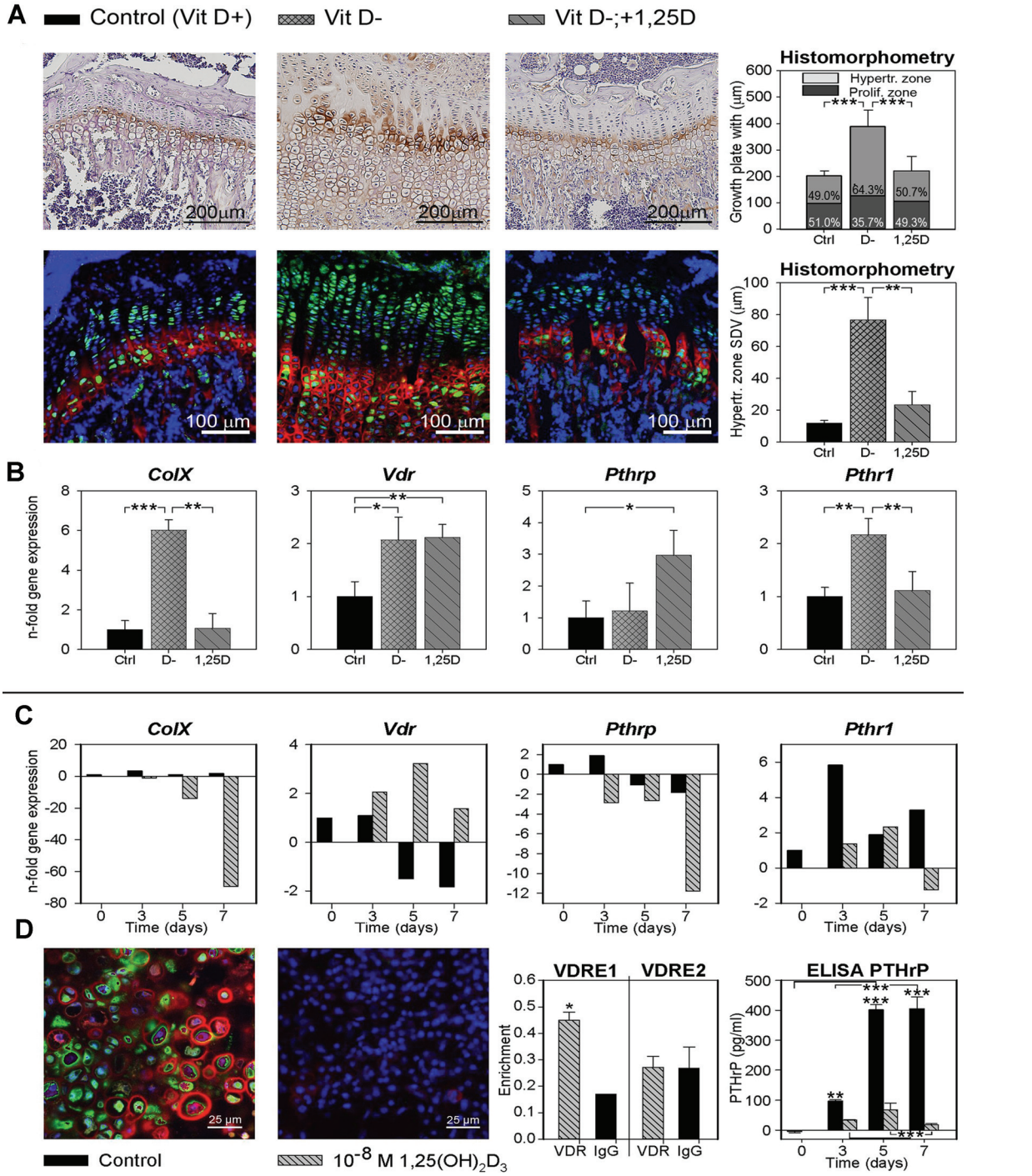

Fig. 7. Results of the in vivo study (A + B) and the primary cell culture (C + D) of Col2-pd2EGFP transgenic mice growth plate chondrocytes. A: Histomorphometry (H&E) and immunofluorescent staining for collagen type X (red) of tibial growth plates from Col2-Col2-pd2EGFP transgenic mice (6 weeks of age) indicating that vitamin D_3 deficient mice (VitD−) developed rickets. Supplementation with 1,25$(OH)_2D_3$ (VitD−;+1,25D) reversed the rachitic phenotype as compared with controls (VitD+). Note that Col2-pd2EGFP fluorescence (green) is native (mean ± SD; n = 7). B: Relative *ColX*, *Vdr*, *Pthrp*, and *Pthr1* gene expression corrected for reference genes in sorted Col2-pd2EGFP positive growth plate chondrocytes after termination of the study, at 6 weeks of age (mean ± SD; n = 6). Relative target gene expression in the growth plate of control (VitD+) mice was set at 1. C: Relative *ColX*, *Vdr*, *Pthrp*, and *Pthr1* gene expression corrected for reference genes in control or 1,25$(OH)_2D_3$-treated cultured primary Col2-pd2EGFP growth plate chondrocytes. Time is shown in days after the start of differentiation (T_0, T_3, T_5, and T_7). From T_2 onward, 10^{-8} M 1,25$(OH)_2D_3$ was daily added to the culture medium. Relative target gene expression at T_0 in the control culture was set at 1. These data were not subjected to statistical analysis due to the small sample size (n = 1 experimental replicate). D: From left to right: Immunofluorescent staining for collagen type X and native expression of Col2-pd2EGFP in control and 10^{-8} M 1,25$(OH)_2D_3$-treated cultured primary Col2-pd2EGFP growth plate chondrocytes. Transcription of collagen type 2 (green) and hypertrophic differentiation of chondrocytes (red) were detected in control cultures, whereas the 10^{-8} M 1,25$(OH)_2D_3$-treated cells expressed no Col2-pd2EGFP and only occasionally collagen type X immunofluorescence in their pericellular matrix. A ChIP assay revealed enrichment of PTHrP VDRE1, but not the VDRE2. A PTHrP ELISA performed on culture media revealed decreased PTHrP production in the 10^{-8} M 1,25$(OH)_2D_3$-treated primary growth plate chondrocytes compared with control cultures (mean ± SD; n = 4). *$P < 0.05$, **$P < 0.01$, ***$P < 0.001$.

Demay, 2002). Their vitamin D_3-deficient phenotype was successfully reversed by 1,25$(OH)_2D_3$ supplementation.

Gene and protein expression of primary growth plate chondrocytes. Col2-pd2EGFP-positive growth plate chondrocytes were sorted and processed for RNA isolation on an individual basis. The number of positive Col2-pd2EGFP chondrocytes was $5.1 \times 10^5 \pm 3.1 \times 10^5$, $1.4 \times 10^6 \pm 8.1 \times 10^5$, and $3.3 \times 10^5 \pm 2.1 \times 10^5$ for the VitD+, VitD−, and VitD−; +1,25D mice, respectively. (Pre) hypertrophic differentiation marker (*ColX* and *Pthr1*) gene expression was significantly higher in VitD− mice than in mice from the two other groups ($P < 0.01$, Fig. 7B). Furthermore, *Vdr* gene expression was significantly higher in VitD− mice than in VitD+ mice ($P < 0.05$) and *Pthrp* gene expression was significantly higher in VitD−; +1,25D mice than in VitD+ mice ($P < 0.05$, Fig. 7B).

Confocal imaging of tibial growth plates from Col2-pd2EGFP transgenic mice indicated that VitD+ and VitD−; +1,25D mice had less Col2-pd2EGFP than VitD− mice (Fig. 7A). Nuclear VDR protein expression was highest in VitD− mice and lowest in VitD+ mice (Supplementary file 6B). Within the proliferative and hypertrophic zones, the percentage area staining for PTHrP (over the total surface of the growth plate, and thus corrected for the larger surface of the growth plate in VitD− mice), the integrated density, and mean gray value did not differ between groups (Supplementary file 6B). However, in accordance with gene expression levels, PTHR1 staining was present in all growth plate zones and seemed to be in greater amounts in VitD− mice than in mice from the other two groups (Supplementary file 6B).

In vitro studies with primary growth plate chondrocytes

As other signaling pathways may interfere with the interpretation of the in vivo results, an in vitro study was performed with primary Col2-pd2EGFP growth plate chondrocytes. Vitamin D_3-deficient primary growth plate chondrocytes (controls) were compared with 10^{-8} M 1,25$(OH)_2D_3$-treated primary growth plate chondrocytes over 7 days. *ColX* gene expression decreased with time and was lower in 1,25$(OH)_2D_3$-treated than in control primary growth plate chondrocytes at all times points (Fig. 7C). In line with our hypothesis, *Pthrp* gene expression was lower and *Vdr* gene expression was higher in 1,25$(OH)_2D_3$-treated compared with control primary growth plate chondrocytes at all time points (Fig. 7C).

Confocal imaging of native Col2-pd2EGFP fluorescence and staining for collagen type X revealed transcription of collagen type II and hypertrophic differentiation of the control cultures at T_7, whereas 1,25$(OH)_2D_3$-treated primary growth plate chondrocytes showed no Col2-pd2EGFP fluorescence and collagen type X staining in their pericellular matrix (Fig. 7D), which was in line with our hypothesis and confirms the reported gene expression profiles.

ChIP assays showed no enrichment of VDRE1, VDRE2, or the negative control in the PTHR1 promoter (data not shown), indicating that there is no functional binding of 1,25$(OH)_2D_3$ and the VDR to a VDRE in the PTHR1 promoter of primary Col2-pd2EGFP growth plate chondrocytes. However, in parallel with what was found in the chondrogenic ATDC5 cell line, ChIP assays on sorted Col2-pd2EGFP growth plate chondrocytes showed a significant 2.6-fold enrichment of VDRE1 ($P < 0.05$), and no enrichment of VDRE2 or the negative control in the PTHrP promoter (Fig. 7D). Furthermore, PTHrP production in 1,25$(OH)_2D_3$-treated primary growth plate chondrocytes was significantly lower than in control cultures at all time points ($P < 0.01$, Fig. 7D). These results indicate that also in primary Col2-pd2EGFP growth plate chondrocytes, 1,25$(OH)_2D_3$ and the VDR together bind to a 1,25$(OH)_2D_3$-responsive region (VDRE1) in the PTHrP promoter. In this way, 1,25$(OH)_2D_3$ directly inhibits PTHrP production via the VDR.

Discussion

The regulation of chondrocyte differentiation is a key event in skeletal development. Regenerative strategies for cartilage engineering use mesenchymal stem cells (MSCs), but are hampered by the inherent capacity of chondrogenically differentiating MSCs to undergo hypertrophic differentiation (Hellingman et al., 2012). Hence, understanding the processes that regulate chondrocyte differentiation is crucial to further fine-tune regenerative strategies for cartilage and bone engineering. In order to do so, we used growth plate chondrocytes, which undergo differentiation in an orderly fashion. We used complementary in vitro (ATDC5 and primary growth plate chondrocytes) and in vivo (Col2-pd2EGFP mice) models and demonstrated that there is a functional paracrine feedback loop between 1,25$(OH)_2D_3$ and PTHrP in prehypertrophic growth plate chondrocytes (Fig. 8).

The effect of PTHrP on the vitamin D_3 pathway

We hypothesized that in growth plate chondrocytes, PTHrP treatment would increase vitamin D_3 activity, either by interference with the key enzymes of vitamin D_3 metabolism (1α- and 24-hydroxylase) or by a direct effect on the VDR (Supplementary File 1). In the kidney, PTH stimulates 1α-hydroxylase and inhibits 24-hydroxylase (Zierold et al., 2003; Xue et al., 2005). The subcutaneous administration of PTHrP to healthy women increased plasma 1,25$(OH)_2D_3$ levels, but did not affect endogenous PTH levels, indicating that—at an

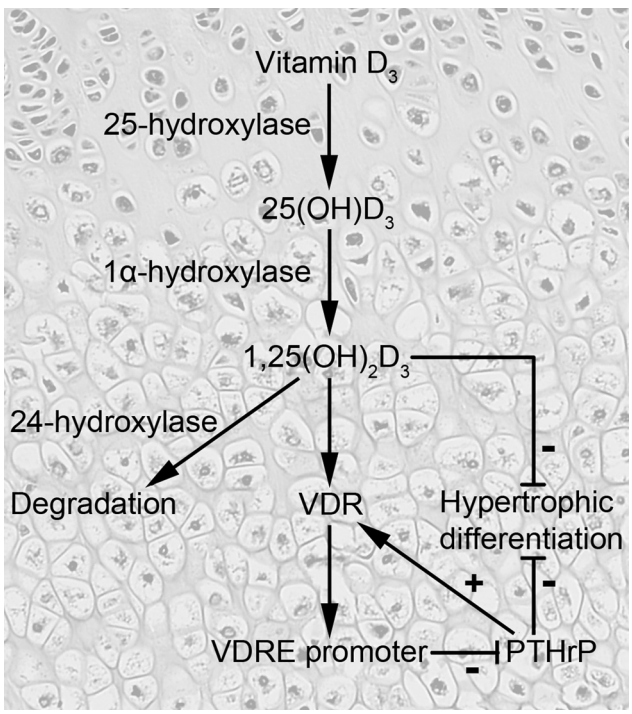

Fig. 8. The paracrine feedback loop between PTHrP and 1,25 $(OH)_2D_3$ in prehypertrophic growth plate chondrocytes. 1,25 $(OH)_2D_3$ inhibits PTHrP production through a VDRE in the PTHrP promoter, and PTHrP increases chondrocyte sensitivity to 1,25 $(OH)_2D_3$ via increased VDR expression.

endocrine level—PTHrP stimulates 1α-hydroxylase in the kidney in the same way that PTH does (Henry et al., 1997). However, in the current study, PTHrP did not significantly affect the expression of 1α- and 24-hydroxylase in ATDC5 chondrocytes in the prehypertrophic phase of differentiation. Although we did not determine the actual activity of the respective enzymes, it is tempting to speculate that PTH and PTHrP influence 1α- and 24-hydroxylase expression in a tissue/cell-specific manner.

We found that PTHrP significantly increased VDR expression (Fig. 1A,B). *Vdr* gene expression was upregulated 4 h after initiation of PTHrP treatment (T_4), whereas repeated treatment resulted in a lower increase in *Vdr* gene expression at T_{28} (Fig. 1A). Desensitization of the PTH-induced cAMP response (Jongen et al., 1996) might explain the decreased response of the ATDC5 cells to PTHrP after the second addition of PTHrP (at T_{24}) compared with the first addition (at T_0). Previous studies found a PTH/PTHrP-mediated decreased VDR expression in renal, intestinal, and osteoblast-like cells (Reinhardt and Horst, 1990; Sriussadaporn et al., 1995; Healy et al., 2005b), but increased VDR expression in growth plate chondrocytes and osteoblast-like cells (Pols et al., 1988; Klaus et al., 1997). A possible explanation for these contradictory results is again a cell-line/tissue specific effect.

The effect of vitamin D_3 on the PTHrP pathway

We hypothesized that treatment with $1,25(OH)_2D_3$ would decrease PTHrP production, because *Pthrp* expression is reported to be suppressed by $1,25(OH)_2D_3$ in several other cell types (Kremer et al., 1991; Falzon, 1996; Sepulveda et al., 2006).

In contrast to our hypothesis, in the in vivo studies with the Col2-pd2EGFP mouse model, *Pthrp* gene expression was increased in Col2-pd2EGFP growth plate chondrocytes from VitD−; +1,25D mice compared with VitD− or VitD+ mice (Fig. 7B). However, these in vivo studies are limited by several factors. First, growth plate chondrocytes were isolated on the basis of FACS of Col2-pd2EGFP-positive chondrocytes and, hence, may not be representative of the total population of growth plate chondrocytes. Second, the altered calcium homeostasis in the vitamin D_3-deficient mice treated with $1,25(OH)_2D_3$ resulted in hypercalcemia (Supplementary file 6A), which could have attributed to the increased *Pthrp* and *Vdr* expression in VitD−; +1,25D mice (Fig. 7B). Calcium has been shown to regulate PTHrP secretion (Kremer et al., 1996b; Chattopadhyay et al., 2000) and to have an additive effect on the homologous upregulation of VDR expression during treatment with $1,25(OH)_2D_3$ (Davoodi et al., 1995; Klaus et al., 1998; Healy et al., 2005a). To exclude the effects of interfering factors, we also performed in vitro studies with ATDC5 and primary Col2-pd2EGFP growth plate chondrocytes and studied the pattern of expression of target genes and proteins in the presence and absence of $1,25(OH)_2D_3$. In line with our hypothesis, PTHrP gene and protein expression was lower in the $1,25(OH)_2D_3$-treated primary Col2-pd2EGFP growth plate chondrocytes compared with control cultures (Fig. 7C,D). Also in prehypertrophic ATDC5 chondrocytes, PTHrP protein production was decreased by $1,25(OH)_2D_3$-treatment (Figs. 1D and 2B,C). The counterintuitive increase of *Pthrp* gene expression in 10^{-8} M $1,25(OH)_2D_3$-treated ATDC5 cultures compared with control cultures from 24 h of treatment onward (Figs. 1C and 2A) could be explained by "*Pthrp* mRNA superinduction" (Ikeda et al., 1990), which is only provoked by the preceding decreased PTHrP protein expression in 10^{-8} M $1,25(OH)_2D_3$-treated prehypertrophic ATDC5 chondrocytes (Fig. 2B,C), and not at lower dosages.

We furthermore silenced the VDR to clarify its role in the regulation of PTHrP expression by $1,25(OH)_2D_3$. VDR silencing counteracted the inhibitory effect of $1,25(OH)_2D_3$ on PTHrP protein production (Fig. 4D). In addition, we observed significant enrichment of the PTHrP VDRE1 in $1,25(OH)_2D_3$-treated ATDC5 and primary growth plate chondrocytes in the prehypertrophic phase of differentiation (Figs. 3B and 7D). This is the first study to report functional binding of $1,25(OH)_2D_3$ through its receptor to the promoter region of the PTHrP gene in growth plate chondrocytes. The $1,25(OH)_2D_3$-responsive region (VDRE) in the PTHrP promoter has already been characterized in other tissues (Kremer et al., 1991, 1996a; Falzon, 1996). Taken together, these findings prove that in the growth plate, the functional paracrine feedback loop between PTHrP and $1,25(OH)_2D_3$ is closed by the inhibition of PTHrP transcription by the binding of $1,25(OH)_2D_3$ to a VDRE located in the PTHrP (and not the PTHR1) promoter region (Fig. 8).

The role of the paracrine PTHrP-$1,25(OH)_2D_3$ feedback loop in hypertrophic chondrocyte differentiation

Having established that there is a functional paracrine feedback loop between PTHrP and $1,25(OH)_2D_3$ in growth plate chondrocytes (Fig. 8), we wanted to define the role of this feedback loop in hypertrophic chondrocyte differentiation. Both $1,25(OH)_2D_3$ and PTHrP affected the proliferation and differentiation of growth plate chondrocytes. $1,25(OH)_2D_3$ treatment resulted in a decreased DNA content of the prehypertrophic ATDC5 chondrocytes, indirectly indicating that $1,25(OH)_2D_3$ had an anti-proliferative effect, which is in line with previous reports (Klaus et al., 1991). Moreover, $1,25(OH)_2D_3$ had an inhibitory effect on chondrocyte hypertrophy, based on the reduced *Col9*, *ColX*, and *Pthr1* gene expression and collagen type X protein expression in $1,25(OH)_2D_3$-treated ATDC5 and primary Col2-pd2EGFP positive growth plate chondrocytes (Figs. 5 and 7C,D). This is by no means a new finding, since $1,25(OH)_2D_3$ has been shown to inhibit terminal chondrocyte differentiation both in vitro and in vivo (Kato et al., 1990; Drissi et al., 2002; Idelevich et al., 2011; Castillo et al., 2012). In addition, VDR silencing in $1,25(OH)_2D_3$-treated ATDC5 cells only partially reversed the anti-hypertrophic effects of $1,25(OH)_2D_3$: it prevented the inhibitory effect of $1,25(OH)_2D_3$ on *Pthr1* gene expression, but it did not affect collagen type X expression (Fig. 6). In unpublished studies, we found that treatment with 10^{-10} and 10^{-12} M $1,25(OH)_2D_3$ decreased the expression of (pre) hypertrophic differentiation markers, and hence VDR silencing may have been ineffective in counteracting the strong inhibitory effect of 10^{-8} M $1,25(OH)_2D_3$ on hypertrophic differentiation. An alternative explanation is that $1,25(OH)_2D_3$ also exerts effects by binding to a membrane-associated receptor PDIA3 (Boyan et al., 2006; St-Arnaud and Naja, 2011).

PTHrP is a well-known suppressor of hypertrophic chondrocyte differentiation (Ballock and O'Keefe, 2003; van der Eerden et al., 2003; Hoogendam et al., 2007; Brochhausen et al., 2009). Accordingly, in the control ATDC5 cultures, *Col9* gene and collagen type X gene and protein expression increased with time, but this increase was prevented by the addition of PTHrP (Fig. 5). Furthermore, the addition of PTHrP to ATDC5 cells in a prehypertrophic differentiation phase significantly downregulated the expression of the gene for the receptor of PTHrP, *Pthr1* (Fig. 5A), which is also in line with previous reports (Weisser et al., 2002; Wealthall, 2009). This homologous downregulation of *Pthr1* is possibly a measure to prevent overstimulation, but another explanation lies in the physiological role of PTHrP, namely, to prevent proliferative cells leaving the proliferating pool. In this way, hypertrophic chondrocyte differentiation—and thus PTHR1 production—is delayed (Kronenberg, 2003; Mak et al., 2008; Hirai et al., 2011; Zhang et al., 2012). Taken together, the results of our study indicate that PTHrP could be used clinically to inhibit

undesirable hypertrophic chondrocyte differentiation. Accordingly, in vitro work has already demonstrated that PTHrP successfully inhibited hypertrophic differentiation of articular chondrocytes (Wang et al., 2011; Zhang et al., 2013) and cartilage constructs engineered from bone marrow-derived mesenchymal stem cells (BMSCs), without losing cartilage-specific matrix proteins (US patent 20080318859, Kafienah et al., 2007). Moreover, in vivo, intra-articular PTHrP injection together with collagen-silk scaffold implantation (4–6 weeks post-injury) inhibited terminal differentiation and enhanced chondrogenesis in induced osteochondral defects in rabbits (Zhang et al., 2013). In contrast, in chondrogenically differentiated BMSC pellets, PTHrP could not diminish the T_3-induced enhancement of hypertrophy (Mueller et al., 2013). Despite significant reduction of some hypertrophic markers, the absolute level of expression was still high compared with articular chondrocyte-based cartilage constructs (Hellingman et al., 2012). Furthermore, PTHrP has even been reported to suppress chondrogenic differentiation of BMSC pellets (Weiss et al., 2010). Noteworthy is the fact that above-mentioned studies started the PTHrP treatment at different time points, that is, before or after manifestation of hypertrophy. Thus, the use of PTHrP needs to be further investigated with regard to the inhibition of hypertrophic chondrocyte differentiation, articular cartilage repair, and the generation of stable engineered cartilage from MSCs (Zhang et al., 2012).

In order to further study how the interaction between 1,25$(OH)_2D_3$ and PTHrP influences hypertrophic chondrocyte differentiation, we evaluated whether PTHrP prevents the differentiation of chondrocytes through a VDR-dependent mechanism. For this purpose, the VDR was successfully silenced in PTHrP-supplemented cultures, but the expression of *Pthr1* gene and collagen type X protein was hardly influenced (Fig. 6). As it is not possible to discuss these results in the light of earlier reports, we can only postulate that the anti-hypertrophic effect of PTHrP is independent of the VDR. This indicates that 1,25$(OH)_2D_3$ and PTHrP individually influence hypertrophic chondrocyte differentiation and thus may have a synergistic effect in suppressing hypertrophic differentiation.

Conclusions

Taken together, the data obtained using an integrative approach involving in vitro studies with ATDC5 and primary growth plate chondrocytes and in vivo studies with Col2-pd2EGFP transgenic mice led us to conclude that there is a functional paracrine feedback loop between PTHrP and 1,25$(OH)_2D_3$ in prehypertrophic growth plate chondrocytes. 1,25$(OH)_2D_3$ inhibits PTHrP production through a functional binding place (VDRE) in the PTHrP promoter, and PTHrP increases chondrocyte sensitivity to 1,25$(OH)_2D_3$ by increasing VDR production (Fig. 8). The results of this study furthermore indicate that 1,25$(OH)_2D_3$ and PTHrP individually influence chondrocyte hypertrophy and, hence, may have the potential to inhibit undesirable hypertrophic chondrocyte differentiation during cartilage repair or engineering. To our knowledge, the effect of 1,25$(OH)_2D_3$ and the synergistic effect of a combination of PTHrP and 1,25$(OH)_2D_3$ on MSC-based cartilage regeneration has not yet been evaluated and might provide leads for new strategies to improve the quality of engineered cartilage.

Acknowledgments

We are very grateful to Rob Bleumink (Center for Cell Imaging) for his assistance with microscopy, Jan Jaap Stevenhagen (TNO Nutrition and Food Research, Zeist, The Netherlands) for the vitamin D_3 content analysis, Ms. Jane Sykes for language corrections, and Mr. Hans Vernooij (Utrecht University, The Netherlands) for assistance in statistical analysis. Furthermore, we thank Dr. G. P. Lunstrum (Oregon Health Sciences University), Dr. T. Welting (UMC Maastricht) and Dr. C. Veldhuizen (Dishman, The Netherlands) for their generous gifts.

Literature Cited

AkenoN, Saikatsu S, Kawane T, Horiuchi N . 1997. Mouse vitamin D-24-hydroxylase: Molecular cloning, tissue distribution, and transcriptional regulation by 1alpha,25-dihydroxyvitamin D3. Endocrinology 138:2233–2240.

Altschul SF, Madden TL, Schaffer AA, Zhang J, Zhang Z, Miller W, Lipman DJ . 1997. Gapped BLAST and PSI-BLAST: A new generation of protein database search programs. Nucleic Acids Res 25:3389–3402.

Altaf FM, Hering TM, Kazmi NH, Yoo JU, Johnstone B . 2006. Ascorbate-enhanced chondrogenesis of ATDC5 cells. Eur Cells Mater 12:64–69.discussion 69–70.

Armbrecht HJ, Boltz MA . 1991. Expression of 25-hydroxyvitamin D 24-hydroxylase cytochrome P450 in kidney and intestine. Effect of 1,25-dihydroxyvitamin D and age. FEBS Lett 292:17–20.

Ballock RT, O'Keefe RJ . 2003. Physiology and pathophysiology of the growth plate. Birth Defects Res C Embryo Today 69:123–143.

Bligh EG, Dyer WJ . 1959. A rapid method of total lipid extraction and purification. Can J Biochem Physiol 37:911–917.

Boyan BD, Sylvia VL, Dean DD, Del Toro F, Schwartz Z . 2002. Differential regulation of growth plate chondrocytes by 1alpha,25-(OH)2D3 and 24R,25-(OH)2D3 involves cell-maturation-specific membrane-receptor-activated phospholipid metabolism. Crit Rev Oral Biol Med 13:143–154.

Boyan BD, Wang L, Wong KL, Jo H, Schwartz Z . 2006. Plasma membrane requirements for 1alpha,25(OH)2D3 dependent PKC signaling in chondrocytes and osteoblasts. Steroids 71:286–290.

Brochhausen C, Lehmann M, Halstenberg S, Meurer A, Klaus G, Kirkpatrick CJ . 2009. Signalling molecules and growth factors for tissue engineering of cartilage-what can we learn from the growth plate. J Tissue Eng Regen Med 3:416–429.

Carlberg C . 1995. Mechanisms of nuclear signalling by vitamin D3. Interplay with retinoid and thyroid hormone signalling. Eur J Biochem 231:517–527.

Caron MM, Emans PJ, Surtel DA, Cremers A, Voncken JW, Welting TJ, van Rhijn LW . 2012. Activation of NF-kappaB/p65 facilitates early chondrogenic differentiation during endochondral ossification. PLoS ONE 7:e33467.

Castillo EC, Hernandez-Cueto MA, Vega-Lopez MA, Lavalle C, Kouri JB, Ortiz-Navarrete V . 2012. Effects of vitamin D supplementation during the induction and progression of osteoarthritis in a rat model. Evid Based Complement Alternat Med 2012:156563.

Chattopadhyay N, Evliyaoglu C, Heese O, Carroll R, Sanders J, Black P, Brown EM . 2000. Regulation of secretion of PTHrP by Ca(2+)-sensing receptor in human astrocytes, astrocytomas, and meningiomas. Am J Physiol Cell Physiol 279:C691–C699.

Davoodi F, Brenner RV, Evans SR, Schumaker LM, Shabahang M, Nauta RJ, Buras RR . 1995. Modulation of vitamin D receptor and estrogen receptor by 1,25(OH)2-vitamin D3 in T-47D human breast cancer cells. J Steroid Biochem Mol Biol 54:147–153.

Denison TA, Koch CF, Shapiro IM, Schwartz Z, Boyan BD . 2009. Inorganic phosphate modulates responsiveness to 24,25(OH)2D3 in chondrogenic ATDC5 cells. J Cell Biochem 107:155–162.

Donohue MM, Demay MB . 2002. Rickets in VDR null mice is secondary to decreased apoptosis of hypertrophic chondrocytes. Endocrinology 143:3691–3694.

Dreier R . 2010. Hypertrophic differentiation of chondrocytes in osteoarthritis: The developmental aspect of degenerative joint disorders. Arthritis Res Ther 12:216.

Drissi H, Pouliot A, Koolloos C, Stein JL, Lian JB, Stein GS, van Wijnen AJ . 2002. 1,25-(OH)2-vitamin D3 suppresses the bone-related Runx2/Cbfa1 gene promoter. Exp Cell Res 274:323–333.

Falzon M . 1996. DNA sequences in the rat parathyroid hormone-related peptide gene responsible for 1,25-dihydroxyvitamin D3-mediated transcriptional repression. Mol Endocrinol 10:672–681.

Healy KD, Zella JB, Prahl JM, DeLuca HF . 2003. Regulation of the murine renal vitamin D receptor by 1,25-dihydroxyvitamin D3 and calcium. Proc Natl Acad Sci USA 100:9733–9737.

Healy KD, Frahm MA, DeLuca HF . 2005a. 1,25-Dihydroxyvitamin D3 up-regulates the renal vitamin D receptor through indirect gene activation and receptor stabilization. Arch Biochem Biophys 433:466–473.

Healy KD, Vanhooke JL, Prahl JM, DeLuca HF . 2005b. Parathyroid hormone decreases renal vitamin D receptor expression in vivo. Proc Natl Acad Sci USA 102:4724–4728.

Hellingman CA, Koevoet W, van Osch GJ . 2012. Can one generate stable hyaline cartilage from adult mesenchymal stem cells? A developmental approach. J Tissue Eng Regen Med 6: e1–e11.

Henry JG, Mitnick M, Dann PR, Stewart AF . 1997. Parathyroid hormone-related protein-(1-36) is biologically active when administered subcutaneously to humans. J Clin Endocrinol Metab 82:900–906.

Hirai T, Chagin AS, Kobayashi T, Mackem S, Kronenberg HM . 2011. Parathyroid hormone/parathyroid hormone-related protein receptor signaling is required for maintenance of the growth plate in postnatal life. Proc Natl Acad Sci USA 108:191–196.

Hoogendam J, Farih-Sips H, van Beek E, Lowik CW, Wit JM, Karperien M . 2007. Novel late response genes of PTHrP in chondrocytes. Horm Res 67:159–170.

Hugel U, Weber L, Reichrath J, Mehls O, Klaus G . 2004. Rat growth plate chondrocytes express low levels of 25-hydroxy-1alpha-hydroxylase. J Steroid Biochem Mol Biol 89-90:143–147.

Idelevich A, Kerschnitzki M, Shahar R, Monsonego-Ornan E . 2011. 1,25(OH)2D3 alters growth plate maturation and bone architecture in young rats with normal renal function. PLoS ONE 6:e20772.

Ikeda K, Lu C, Weir EC, Mangin M, Broadus AE . 1990. Regulation of parathyroid hormone-related peptide gene expression by cycloheximide. J Biol Chem 265:5398–5402.

Jongen JW, Willemstein-van Hove EC, van der Meer JM, Bos MP, Juppner H, Segre GV, Abou-Samra AB, Feyen JH, Herrmann-Erlee MP . 1996. Down-regulation of the receptor for parathyroid hormone (PTH) and PTH-related peptide by PTH in primary fetal rat osteoblasts. J Bone Miner Res 11:1218–1225.

Kafienah W, Mistry S, Dickinson SC, Sims TJ, Learmonth I, Hollander AP . 2007. Three-dimensional cartilage tissue engineering using adult stem cells from osteoarthritis patients. Arthritis Rheum 56:177–187.

Kato Y, Shimazu A, Iwamoto M, Nakashima K, Koike T, Suzuki F, Nishii Y, Sato K . 1990. Role of 1,25-dihydroxycholecalciferol in growth-plate cartilage: Inhibition of terminal differentiation of chondrocytes in vitro and in vivo. Proc Natl Acad Sci USA 87:6522–6526.
Klaus G, Meinhold-Heerlein R, Milde P, Ritz E, Mehls O . 1991. Effect of vitamin D on growth cartilage cell proliferation in vitro. Pediatr Nephrol 5:461–466.
Klaus G, May T, Hugel U, von Eichel B, Rodriguez J, Fernandez P, Reichrath J, Ritz E, Mehls O . 1997. Parathyroid hormone prevents 1,25 (OH)2D3 induced down-regulation of the vitamin D receptor in growth plate chondrocytes in vitro. Kidney Int 52:45–51.
Klaus G, Weber L, Rodriguez J, Fernandez P, Klein T, Grulich-Henn J, Hugel U, Ritz E, Mehls P . 1998. Interaction of IGF-I and 1 alpha, 25(OH)2D3 on receptor expression and growth stimulation in rat growth plate chondrocytes. Kidney Int 53:1152–1161.
Kremer R, Karaplis AC, Henderson J, Gulliver W, Banville D, Hendy GN, Goltzman D . 1991. Regulation of parathyroid hormone-like peptide in cultured normal human keratinocytes. Effect of growth factors and 1,25 dihydroxyvitamin D3 on gene expression and secretion. J Clin Invest 87:884–893.
Kremer R, Sebag M, Champigny C, Meerovitch K, Hendy GN, White J, Goltzman D . 1996a. Identification and characterization of 1,25-dihydroxyvitamin D3-responsive repressor sequences in the rat parathyroid hormone-related peptide gene. J Biol Chem 271:16310–16316.
Kremer R, Woodworth CD, Goltzman D . 1996b. Expression and action of parathyroid hormone-related peptide in human cervical epithelial cells. Am J Physiol 271:C164–C171.
Kronenberg HM . 2003. Developmental regulation of the growth plate. Nature 423:332–336.
Lunstrum GP, Keene DR, Weksler NB, Cho YJ, Cornwall M, Horton WA . 1999. Chondrocyte differentiation in a rat mesenchymal cell line. J Histochem Cytochem 47:1–6.
Mak KK, Kronenberg HM, Chuang PT, Mackem S, Yang Y . 2008. Indian hedgehog signals independently of PTHrP to promote chondrocyte hypertrophy. Development 135:1947–1956.
Mueller MB, Fischer M, Zellner J, Berner A, Dienstknecht T, Kujat R, Prantl L, Nerlich M, Tuan RS, Angele P . 2013. Effect of parathyroid hormone-related protein in an in vitro hypertrophy model for mesenchymal stem cell chondrogenesis. Int Orthop 37:945–951.
Naja RP, Dardenne O, Arabian A, St Arnaud R . 2009. Chondrocyte-specific modulation of Cyp27b1 expression supports a role for local synthesis of 1,25-dihydroxyvitamin D3 in growth plate development. Endocrinology 150:4024–4032.
Nilsson O, Marino R, De Luca F, Phillip M, Baron J . 2005. Endocrine regulation of the growth plate. Horm Res 64:157–165.
Pandit SK, Westendorp B, Nantasanti S, van Liere E, Tooten PC, Cornelissen PW, Toussaint MJ, Lamers WH, de Bruin A . 2012. E2F8 is essential for polyploidization in mammalian cells. Nat Cell Biol 14:1181–1191.
Persengiev SP, Zhu X, Green MR . 2004. Nonspecific, concentration-dependent stimulation and repression of mammalian gene expression by small interfering RNAs (siRNAs). RNA 10:12–18.
Pfaffl MW . 2001. A new mathematical model for relative quantification in real-time RT-PCR. Nucleic Acids Res 29:e45.
Pols H, van Leeuwen JP, Schilte JP, Visser TJ, Birkenhäger JC. 1988. Heterologous up-regulation of the 1,25-dihydroxyvitamin D3 receptor by parathyroid hormone (PTH) and PTH-like peptide in osteoblast-like cells. Biochem Biophys Res Commun 156:588–594.
R Core Team . 2012. R: A language and environment for statistical computing. Vienna, Austria: R Foundation for Statistical Computing .ISBN 3-900051-07-0.
Reinhardt TA, Horst RL . 1990. Parathyroid hormone down-regulates 1,25-dihydroxyvitamin D receptors (VDR) and VDR messenger ribonucleic acid in vitro and blocks homologous up-regulation of VDR in vivo. Endocrinology 127:942–948.
Reinhardt TA, Horst RL, Orf JW, Hollis BW . 1984. A microassay for 1,25-dihydroxyvitamin D not requiring high performance liquid chromatography: Application to clinical studies. J Clin Endocrinol Metab 58:91–98.
Schipani E, Provot S . 2003. PTHrP, PTH, and the PTH/PTHrP receptor in endochondral bone development. Birth Defects Res C Embryo Today 69:352–362.
Sepulveda VA, Weigel NL, Falzon M . 2006. Prostate cancer cell type-specific involvement of the VDR and RXR in regulation of the human PTHrP gene via a negative VDRE. Steroids 71:102–115.
Sriussadaporn S, Wong MS, Whitfield JF, Tembe V, Favus MJ . 1995. Structure-function relationship of human parathyroid hormone in the regulation of vitamin D receptor expression in osteoblast-like cells (ROS 17/2.8). Endocrinology 136:3735–3742.
St-Arnaud R, Naja RP . 2011. Vitamin D metabolism, cartilage and bone fracture repair. Mol Cell Endocrinol 347:48–54.
Toell A, Polly P, Carlberg C . 2000. All natural DR3-type vitamin D response elements show a similar functionality in vitro. Biochem J 352:301–309.
Tryfonidou MA, Oosterlaken-Dijksterhuis MA, Mol JA, van den Ingh TS, van den Brom WE, Hazewinkel HA . 2003. 24-Hydroxylase: Potential key regulator in hypervitaminosis D3 in growing dogs. Am J Physiol Endocrinol Metab 284:E505–E513.
Tryfonidou MA, Lunstrum GP, Hendriks K, Riemers FM, Wubbolts R, Hazewinkel HA, Degnin CR, Horton WA . 2011. Novel type II collagen reporter mice: New tool for assessing collagen 2alpha1 expression in vivo and in vitro. Dev Dyn 240:663–673.
van der Eerden BC, Karperien M, Wit JM . 2003. Systemic and local regulation of the growth plate. Endocr Rev 24:782–801.
van der Kraan PM, van den Berg WB . 2012. Chondrocyte hypertrophy and osteoarthritis: Role in initiation and progression of cartilage degeneration? Osteoarthritis Cartilage 20:223–232.
Vandesompele J, De Preter K, Pattyn F, Poppe B, Van Roy N, De Paepe A, Speleman F . 2002. Accurate normalization of real-time quantitative RT-PCR data by geometric averaging of multiple internal control genes. Genome Biol 3:RESEARCH0034.
Wang D, Taboas JM, Tuan RS . 2011. PTHrP overexpression partially inhibits a mechanical strain-induced arthritic phenotype in chondrocytes. Osteoarthritis Cartilage 19:213–221.
Wealthall RJ . 2009. In vitro regulation of proliferation and differentiation within a postnatal growth plate of the cranial base by parathyroid hormone-related peptide (PTHrP). J Cell Physiol 219:688–697.
Weiss S, Hennig T, Bock R, Steck E, Richter W . 2010. Impact of growth factors and PTHrP on early and late chondrogenic differentiation of human mesenchymal stem cells. J Cell Physiol 223:84–93.
Weisser J, Riemer S, Schmidl M, Suva LJ, Poschl E, Brauer R, von der Mark K . 2002. Four distinct chondrocyte populations in the fetal bovine growth plate: Highest expression levels of PTH/PTHrP receptor, Indian hedgehog, and MMP-13 in hypertrophic chondrocytes and their suppression by PTH (1–34) and PTHrP (1-40). Exp Cell Res 279:1–13.
Xue Y, Karaplis AC, Hendy GN, Goltzman D, Miao D . 2005. Genetic models show that parathyroid hormone and 1,25-dihydroxyvitamin D3 play distinct and synergistic roles in postnatal mineral ion homeostasis and skeletal development. Hum Mol Genet 14:1515–1528.
Zhang W, Chen J, Zhang S, Ouyang HW . 2012. Inhibitory function of parathyroid hormone-related protein on chondrocyte hypertrophy: The implication for articular cartilage repair. Arthritis Res Ther 14:221.
Zhang W, Chen J, Tao J, Hu C, Chen L, Zhao H, Xu G, Heng BC, Ouyang HW . 2013. The promotion of osteochondral repair by combined intra-articular injection of parathyroid hormone-related protein and implantation of a bi-layer collagen-silk scaffold. Biomaterials 34:6046–6057.
Zierold C, Darwish HM, DeLuca HF . 1995. Two vitamin D response elements function in the rat 1,25-dihydroxyvitamin D 24-hydroxylase promoter. J Biol Chem 270:1675–1678.
Zierold C, Mings JA, DeLuca HF . 2003. Regulation of 25-hydroxyvitamin D3-24-hydroxylase mRNA by 1,25-dihydroxyvitamin D3 and parathyroid hormone. J Cell Biochem 88:234–237.
Zuker M . 2003. Mfold web server for nucleic acid folding and hybridization prediction. Nucleic Acids Res 31:3406–3415.

Supporting Information

Additional supporting information may be found in the online version of this article at the publisher's web-site.